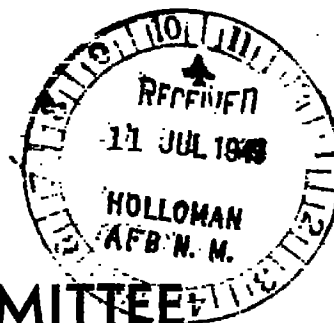# NACA

RESEARCH MEMORANDUM

THE AERODYNAMIC CHARACTERISTICS THROUGHOUT THE

SUBSONIC SPEED RANGE OF A THIN, SHARP-EDGED

HORIZONTAL TAIL OF ASPECT RATIO 4 EQUIPPED

WITH A CONSTANT-CHORD ELEVATOR

By Angelo Bandettini and Verlin D. Reed

Ames Aeronautical Laboratory
Moffett Field, Calif.

NATIONAL ADVISORY COMMITTEE
FOR AERONAUTICS

WASHINGTON
June 30, 1949

NATIONAL ADVISORY COMMITTEE FOR AERONAUTICS

RESEARCH MEMORANDUM

THE AERODYNAMIC CHARACTERISTICS THROUGHOUT THE SUBSONIC SPEED

RANGE OF A THIN, SHARP-EDGED HORIZONTAL TAIL OF ASPECT

RATIO 4 EQUIPPED WITH A CONSTANT-CHORD ELEVATOR

By Angelo Bandettini and Verlin D. Reed

SUMMARY

Wind-tunnel tests have been made of a semispan model of a hori-
zontal tail of aspect ratio 4 and taper ratio 0.5 equipped with a
full-span constant-chord elevator having an area equal to 20 percent
of the total semispan-tail area. The horizontal tail was not swept
and the profile was a sharp-edged, faired double wedge with a
thickness-chord ratio of 0.042. Lift, drag, and pitching-moment
data are presented for a Reynolds number of 2,000,000 at Mach numbers
from 0.20 to 0.94.

At small angles of attack and small elevator deflections, the
effect of compressibility on the effectiveness of the elevator in
producing lift was small at Mach numbers less than 0.60. There was
a gradual increase in effectiveness between Mach numbers of 0.60 and
0.90 to a value equal to 146 percent of the low-speed value. At higher
Mach numbers the effectiveness decreased slightly to a value at a Mach
number of 0.94 equal to 127 percent of the low-speed value. The
variation of lift coefficient with elevator deflection was not linear,
the effectiveness being lower for deflections from 0° to 2° than for
deflections from 2° to 4°. Neither the magnitude nor extent of this
nonlinearity in effectiveness at small elevator deflections was
aggravated by compressibility.

INTRODUCTION

Recent investigations have indicated several wing plan forms,
wing sections, and wing-body-tail combinations suitable for flight
at supersonic speeds. One such lifting surface, a thin, sharp-edged
wing without sweep of aspect ratio 4 and taper ratio 0.5, has been

the subject of an investigation in the Ames 12-foot pressure wind tunnel. The aim of the investigation was to determine the aerodynamic characteristics of such a wing plan form throughout the range of subsonic Mach numbers up to 0.94. Various phases of the investigation have been reported in references 1, 2, 3, and 4. Application of the data of these references to a wing-body-tail combination indicated the possibility of obtaining adequate longitudinal control throughout the speed range by using either an all-movable stabilizer or an adjustable stabilizer with an elevator. To provide data on the effectiveness of an elevator applied to such a plan form, the model previously tested as a wing has been tested as a horizontal tail with a full-span elevator. The tests were conducted at a constant Reynolds number of 2,000,000 at Mach numbers from 0.20 to 0.94.

COEFFICIENTS AND SYMBOLS

The following coefficients are used in this report:

C_L lift coefficient $\left(\dfrac{lift}{qS}\right)$

C_D drag coefficient $\left(\dfrac{drag}{qS}\right)$

C_m pitching-moment coefficient about quarter-chord point

of the mean aerodynamic chord $\left(\dfrac{pitching\ moment}{qS\bar{c}}\right)$

The following symbols are used in this report:

a   speed of sound, feet per second

b   twice model semispan, feet

c   local chord, feet

$\bar{c}$ mean aerodynamic chord, chord through centroid of

semispan plan-form area $\left(\dfrac{\int_0^{b/2} c^2\ dy}{\int_0^{b/2} c\ dy}\right)$,   feet

M   Mach number $\left(\dfrac{V}{a}\right)$

q   free-stream dynamic pressure $\left(\dfrac{\rho V^2}{2}\right)$,   pounds per square
           foot

R   Reynolds number $\left(\dfrac{\rho \bar{V} c}{\mu}\right)$

S   area of semispan tail, square feet

V   airspeed, feet per second

y   distance from plane of symmetry to any spanwise station, feet

α angle of attack of tail-chord plane, degrees

δ_e elevator deflection, positive to increase lift, degrees

μ viscosity of air, slugs per foot-second

ρ mass density of air, slugs per cubic foot

C_{L_α} $\left(\dfrac{\partial C_L}{\partial \alpha}\right)_{\delta=0^\circ}$, measured at $\alpha=0^\circ$

$C_{L_\delta}{}^*$ $\left(\dfrac{C_{L_{\delta=4^\circ}} - C_{L_{\delta=0^\circ}}}{4}\right)_{\alpha=0^\circ}$

α_δ $-\left(\dfrac{C_{L_\delta}{}^*}{C_{L_\alpha}}\right)_{C_L=0}$

(The subscripts outside the parenthesis indicate the factor held constant during the measurement of the parameters.)

MODEL AND APPARATUS

The tests were conducted in the Ames 12-foot pressure wind tunnel. The horizontal tail with full-span elevator used in this investigation was the same model as that used in the tests reported in reference 1. The semispan model represented a tail of aspect ratio 4 and taper ratio 0.5. The 50-percent-chord line of the tail was normal to the plane of symmetry and the airfoil profile was a sharp-edged, symmetrical, faired double wedge with a thickness-chord ratio of 0.042. The constant-chord elevator had an area equal to 20 percent of the total semispan tail area. The unsealed gap between the elevator and the tail was 0.015 inch. Dimensions of the model are given in figure 1. The semispan model was mounted vertically in the tunnel as shown in figure 2. The leading-edge flap with which the model was equipped remained undeflected throughout the present series of tests and all surface roughness

associated with the leading-edge flap and its angle brackets was minimized by sealing the gap and smoothing the surface. The elevator was attached to the tail by hinges and rigidly held in position by steel angle plates. Angular distortion of the elevator due to aerodynamic loads was negligible.

CORRECTIONS TO DATA

The data of this investigation have been corrected for tunnel-wall interference, constriction due to the tunnel walls, and model-support tare forces. The method of reference 5 was used in correcting the data for tunnel-wall interference. The following corrections were added:

$$\Delta\alpha = 0.363 \ C_L$$

$$\Delta C_D = 0.0056 \ C_L^2$$

$$\Delta C_m = 0$$

Corrections to the data for constriction effects of the tunnel walls have been evaluated by the method of reference 6. The magnitude of these corrections as applied to Mach number and to dynamic pressure (measured with the tunnel empty) is illustrated by the following table:

Corrected Mach number	Uncorrected Mach number	$\dfrac{q_{corrected}[1]}{q_{uncorrected}}$
0.94	0.931	1.004
.92	.915	1.003
.90	.897	1.002
.87	.868	1.002
.85	.848	1.002
.80	.799	1.001
.70	.700	1.001
.50	.500	1.001
.20	.200	1.001

[1]The values of $q_{corrected}/q_{uncorrected}$ which were presented in references 1, 3, and 4, were erroneously tabulated and were not the values used in the reduction of the data. The correct values are presented herein and are the values which were actually applied to all test data on this model.

Tare corrections due to the air forces exerted on the exposed
area of the turntable were obtained from force measurements made with
the model removed from the tunnel. Possible interference effects
between the model and the turntable were not evaluated but they are
believed to be small. The magnitude of the measured tare drag coef-
ficient was 0.0063.

TESTS

Lift, drag, and pitching-moment data have been obtained for a
range of angle of attack at a constant Reynolds number of 2,000,000
and Mach numbers from 0.20 to 0.94. For each angle of attack and
Mach number, tests were made with elevator deflections of 0°, 2°, 4°,
6°, 10°, 20°, and 30° except at a Mach number of 0.94 where the
maximum elevator deflection was limited to 20°. At low speeds, the
angle-of-attack range was from -15° to 15°, but at Mach numbers above
0.85 the range was limited by tunnel power and model strength.

RESULTS AND DISCUSSION

Lift, drag, and pitching-moment characteristics as a function
of angle of attack are presented in figures 3 to 11, inclusive, for
elevator deflections of 0°, 2°, 4°, 6°, 10°, 20°, and 30° at Mach
numbers of 0.20, 0.50, 0.70, 0.80, 0.85, 0.87, 0.90, 0.92, and 0.94.
Since the tail profile is symmetrical, the data presented in these
figures for positive elevator deflections can be used to indicate
the effect of negative elevator deflections by simply reversing
the algebraic signs of the coordinate axes. The variation of lift
coefficient with elevator deflection for various Mach numbers is
shown in figure 12 and the lift data are plotted in figures 13 and
14 as a function of Mach number.

Lift Characteristics

Stabilizer effectiveness.— The aerodynamic characteristics of
the horizontal tail with the elevator neutral (figs. 3 to 11, inclusive)
have been fully reported in reference 1. Despite the symmetry of the
profile, the character of the stall with the elevator neutral was
dependent on the algebraic sign of the angle of attack. This is
especially noticeable at a Mach number of 0.80 (fig. 6) where the
tail stalled abruptly with a sizable loss of lift at 8° angle of
attack, but had a gentle stall with a relatively small loss of lift
at about -12° angle of attack. This asymmetry may be due in part to

a small inadvertent deflection of the leading-edge flap or to
differences in the surface roughness of the upper and lower surfaces
as a result of the flap angle brackets. Except at the Mach number
of 0.80, the variation of lift coefficient with angle of attack with
the elevator neutral was nearly symmetrical about the angle of zero
lift. At Mach numbers of 0.80 and 0.85 with the elevator neutral,
the tail stalled abruptly with a sizable loss of lift; whereas at
Mach numbers less than 0.80 the lift curve was rounded at the stall.
The Mach number at which the type of stall changed was affected to
some extent by the Reynolds number as can be seen from the data of
reference 1.

The effect of compressibility on the lift-curve slope with the
elevator neutral is shown in figure 15. The lift-curve slope increased
from 0.062 to 0.095 as the Mach number increased from 0.20 to 0.94.

Elevator effectiveness.— The variation of lift coefficient with
elevator deflection for various Mach numbers is shown in figure 12.
At deflections between 0° and 2°, the elevator effectiveness was
generally lower than for deflections between 2° and 4°. Neither the
magnitude nor the extent of this reduced effectiveness at deflections
near zero was aggravated by compressibility. At a Mach number of 0.20,
the elevator effectiveness was approximately linear from 2° to 15°
with a value of slope $\partial C_L/\partial \delta$ of 0.034. The value of $\partial C_L/\partial \delta$
predicted from thin-airfoil theory (reference 7), assuming the experi-
mental value of tail lift-curve slope, was 0.035.

The effects of compressibility on the elevator effectiveness
parameters are presented in figure 15 where $C_{L_\delta}{}^*$ and α_δ are shown
as functions of Mach number. Due to the nonlinearity of the variation
of the lift coefficient with elevator deflection for small elevator
deflections, the effectiveness parameter $C_{L_\delta}{}^*$ was obtained as the
difference in the lift coefficient due to 4° of elevator deflection
divided by 4. The value of $C_{L_\delta}{}^*$ was 0.030 and was not affected by
compressibility at Mach numbers less than 0.60. As the Mach number
was increased to 0.90, $C_{L_\delta}{}^*$ increased to 0.044, subsequently decreas-
ing to 0.038 at a Mach number of 0.94.

To demonstrate more clearly the effects of compressibility on the
elevator effectiveness, the variation of lift coefficient with Mach
number for various angles of attack of the tail with constant elevator
deflections is presented in figure 13, and the variation of lift coef-
ficient with Mach number for various elevator deflections at constant
angles of attack is presented in figure 14. In figure 14, the data
obtained with a positive elevator deflection and a negative angle of

attack are presented as data for negative elevator deflections at a
positive angle of attack.

Drag Characteristics

The effects of elevator deflection on the drag characteristics
of the horizontal tail are shown in figures 3 to 11, inclusive. At
Mach numbers less than 0.80 the minimum drag coefficient was little
affected by elevator deflection for deflections up to 6°. At elevator
deflections greater than 6°, the minimum drag coefficient increased
with increasing elevator deflection at all Mach numbers. At all Mach
numbers less than 0.92, the maximum lift–drag ratio was increased
slightly by small deflections of the elevator.

Pitching–Moment Characteristics

The effects of elevator deflection on the pitching–moment charac-
teristics of the horizontal tail are presented in figure 3 to 11,
inclusive. At a Mach number of 0.20, there was a marked rearward
movement of the aerodynamic center starting at an angle of attack of
approximately 6°. The angle of attack at which this movement started
was not affected by elevator deflection. As the Mach number increased,
the extent of the rearward movement was reduced and occurred at
slightly smaller angles of attack. The effect of elevator deflection
on the pitching–moment coefficient was strongly affected by compressi-
bility. At a Mach number of 0.20, the pitching–moment coefficient at
zero lift due to 6° of elevator deflection was –0.056. With this
same elevator deflection and at a Mach number of 0.94, the pitching–
moment coefficient at zero lift was –0.120, an increase of 114 percent.
Similar increases in pitching–moment coefficient with increasing Mach
number are apparent for all elevator deflections.

Ames Aeronautical Laboratory,
    National Advisory Committee for Aeronautics,
        Moffett Field, Calif.

REFERENCES

1. Johnson, Ben H., Jr.: Investigation of a Thin Wing of Aspect
   Ratio 4 in the Ames 12-Foot Pressure Wind Tunnel. I — Charac-
   teristics of a Plain Wing. NACA RM A8D07, 1948.

2. Johnson, Ben H., Jr., and Bandettini, Angelo: Investigation of a
   Thin Wing of Aspect Ratio 4 in the Ames 12-Foot Pressure Wind
   Tunnel. II — The Effect of Constant-Chord Leading- and Trailing-
   Edge Flaps on the Low-Speed Characteristics of the Wing.
   NACA RM A8F15, 1948.

3. Johnson, Ben H., Jr., and Demele, Fred A.: Investigation of a
   Thin Wing of Aspect Ratio 4 in the Ames 12-Foot Pressure Wind
   Tunnel. III — The Effectiveness of a Constant-Chord Aileron.
   NACA RM A8I17, 1948.

4. Johnson, Ben H., Jr., and Reed, Verlin D.: Investigation of a
   Thin Wing of Aspect Ratio 4 in the Ames 12-Foot Pressure Wind
   Tunnel. IV — The Effect of a Constant-Chord Leading-Edge
   Flap at High Subsonic Speeds. NACA RM A8K19, 1949.

5. Sivells, James C., and Deters, Owen J.: Jet-Boundary and Plan-
   Form Corrections for Partial-Span Models with Reflection
   Plane, End Plate, or no End Plate, in a Closed Circular Wind
   Tunnel. NACA TN 1077, 1946.

6. Herriot, John G.: Blockage Corrections for Three-Dimensional-
   Flow Closed-Throat Wind Tunnels, with Consideration of the
   Effect of Compressibility. NACA RM A7B28, 1947.

7. Allen, H. Julian: Calculation of the Chordwise Load Distribution
   over Airfoil Sections with Plain, Split, or Serially Hinged
   Trailing-Edge Flaps. NACA Rep. 634, 1938.

All dimensions
given in inches
unless otherwise
specified.

Elevator
hinge line

12.00

Moment
center, $\frac{\bar{c}}{4}$

$\bar{c}$ = 18.67

36.00

16.00

3.55

24.00
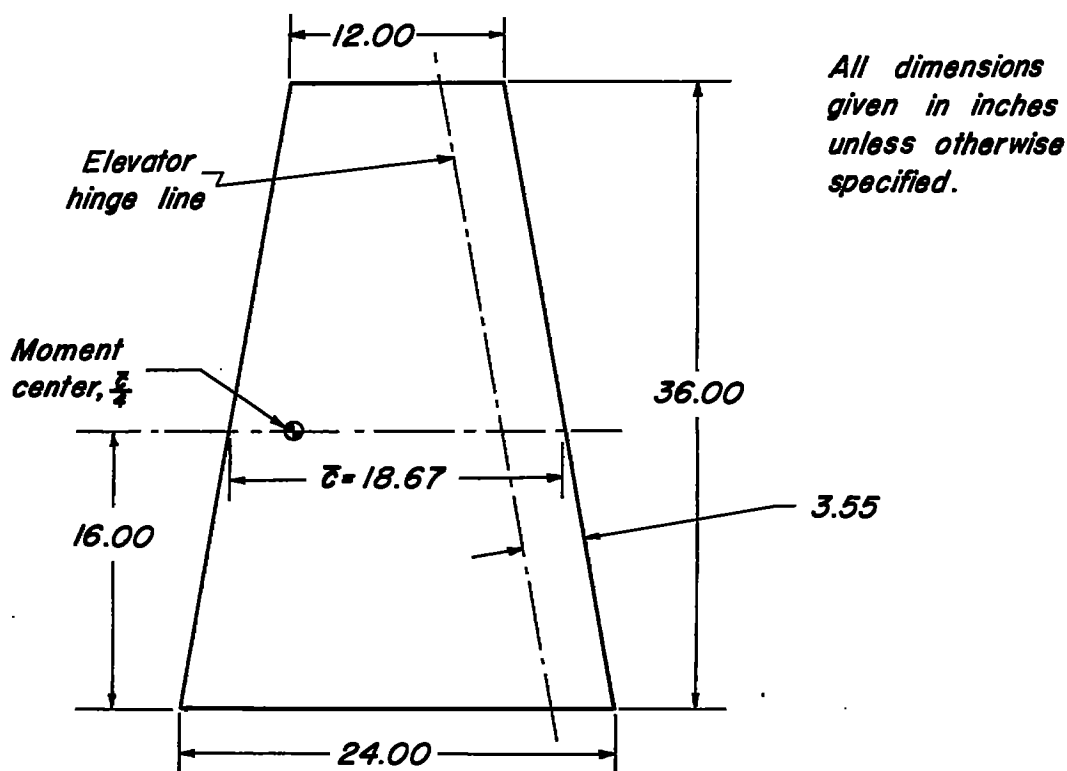
Tail plan form

Note: Leading – and trailing –
edge radii are 0.005.

R = 1.686 c

.015 gap

.042 c   .045 c   5.1°

.500 c

.150 c

c
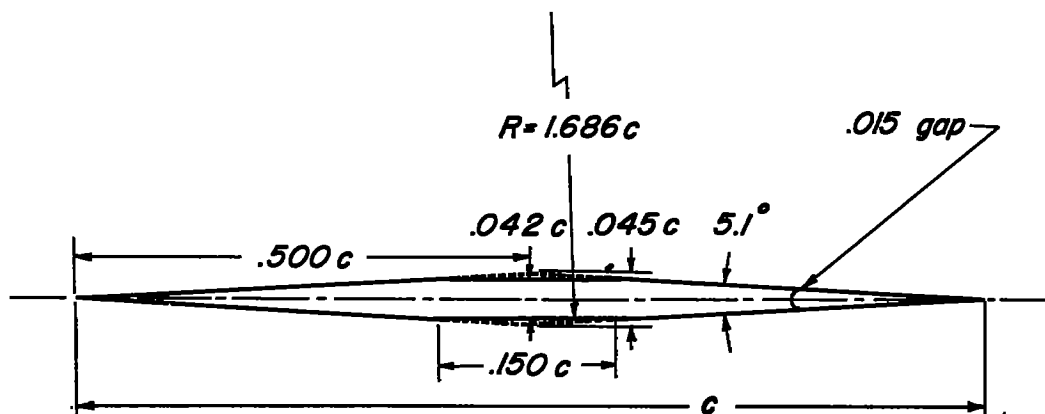
Typical section, symmetrical faired double wedge

Figure 1.— Semispan model of a horizontal tail of aspect ratio 4
tested in the Ames 12 – foot pressure wind tunnel.

Figure 2.— Semispan model of a horizontal tail of aspect ratio 4 mounted in the Ames 12—foot pressure wind tunnel.
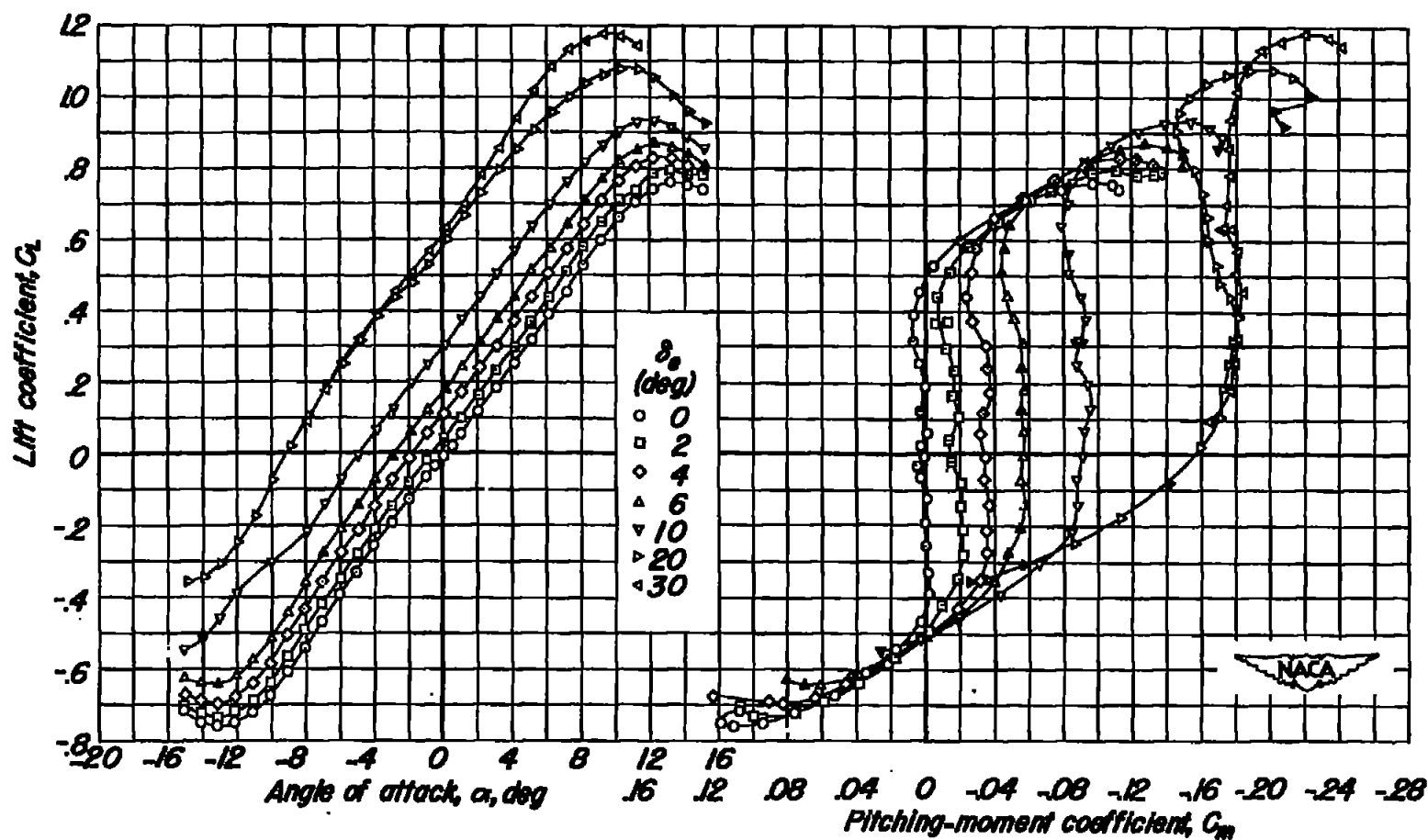
(a) C_L vs α, C_L vs C_m.

Figure 3. — The effect of elevator deflection on the aerodynamic characteristics of the tail at a Mach number of 0.20.
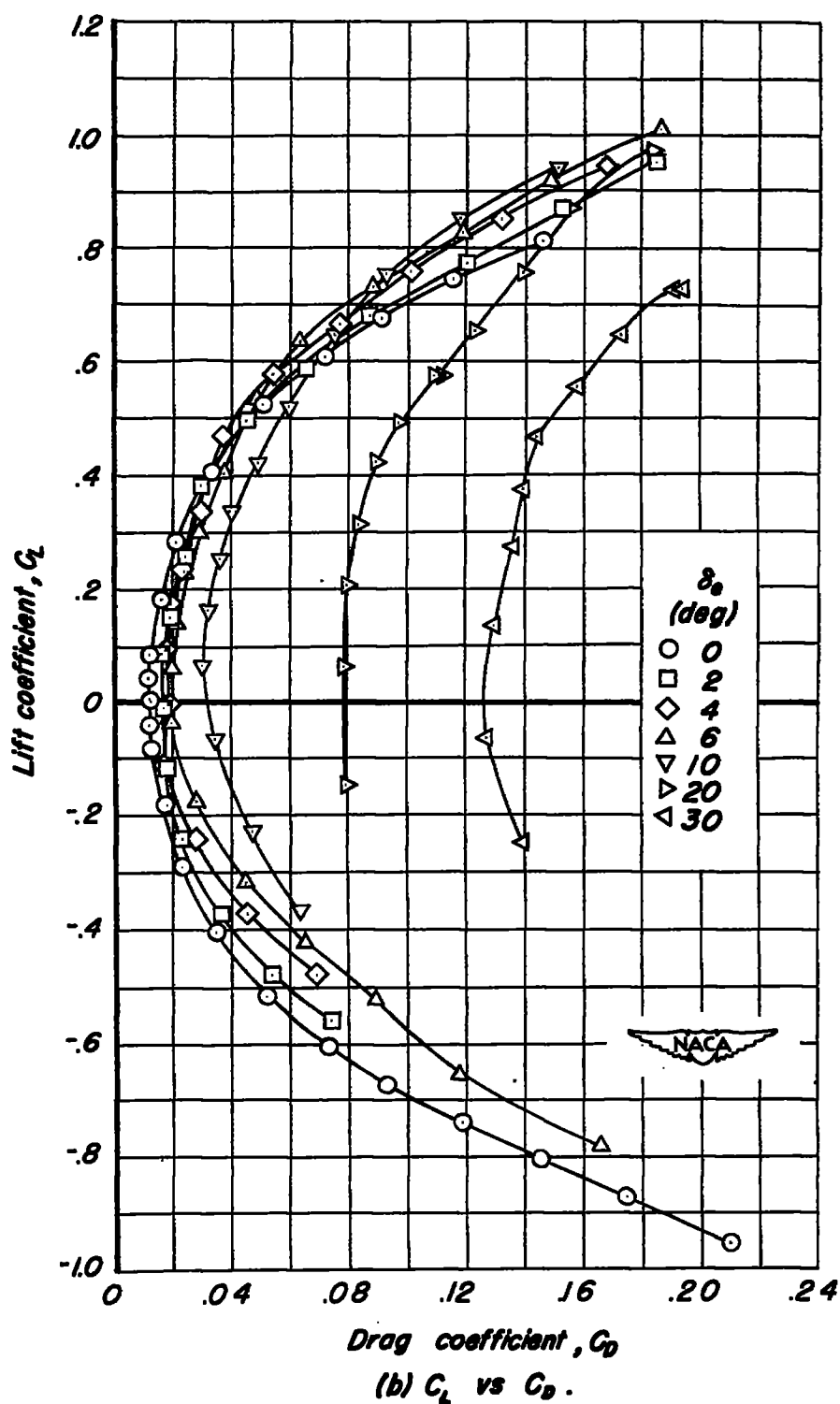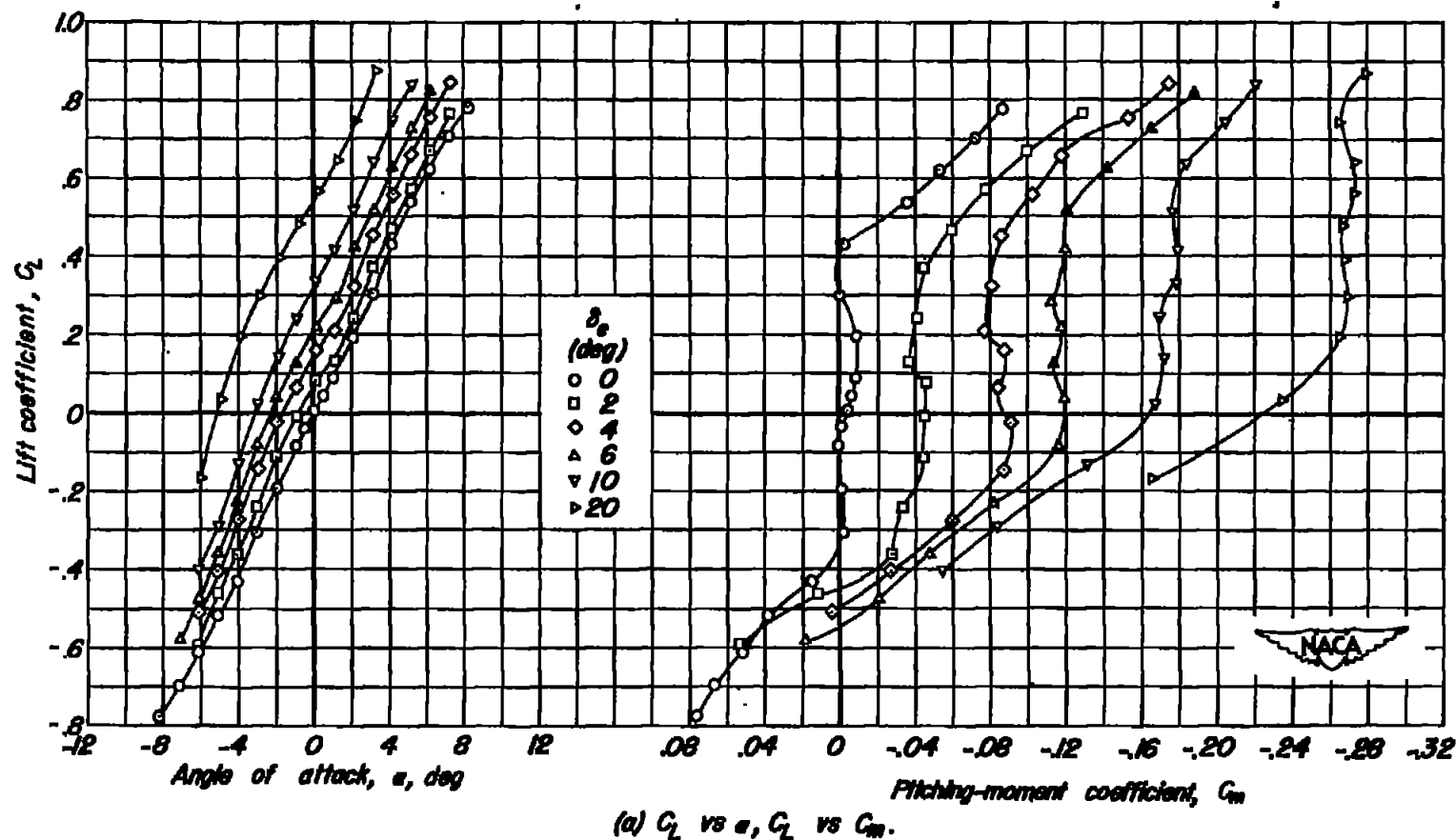
(b) C_L vs C_D.
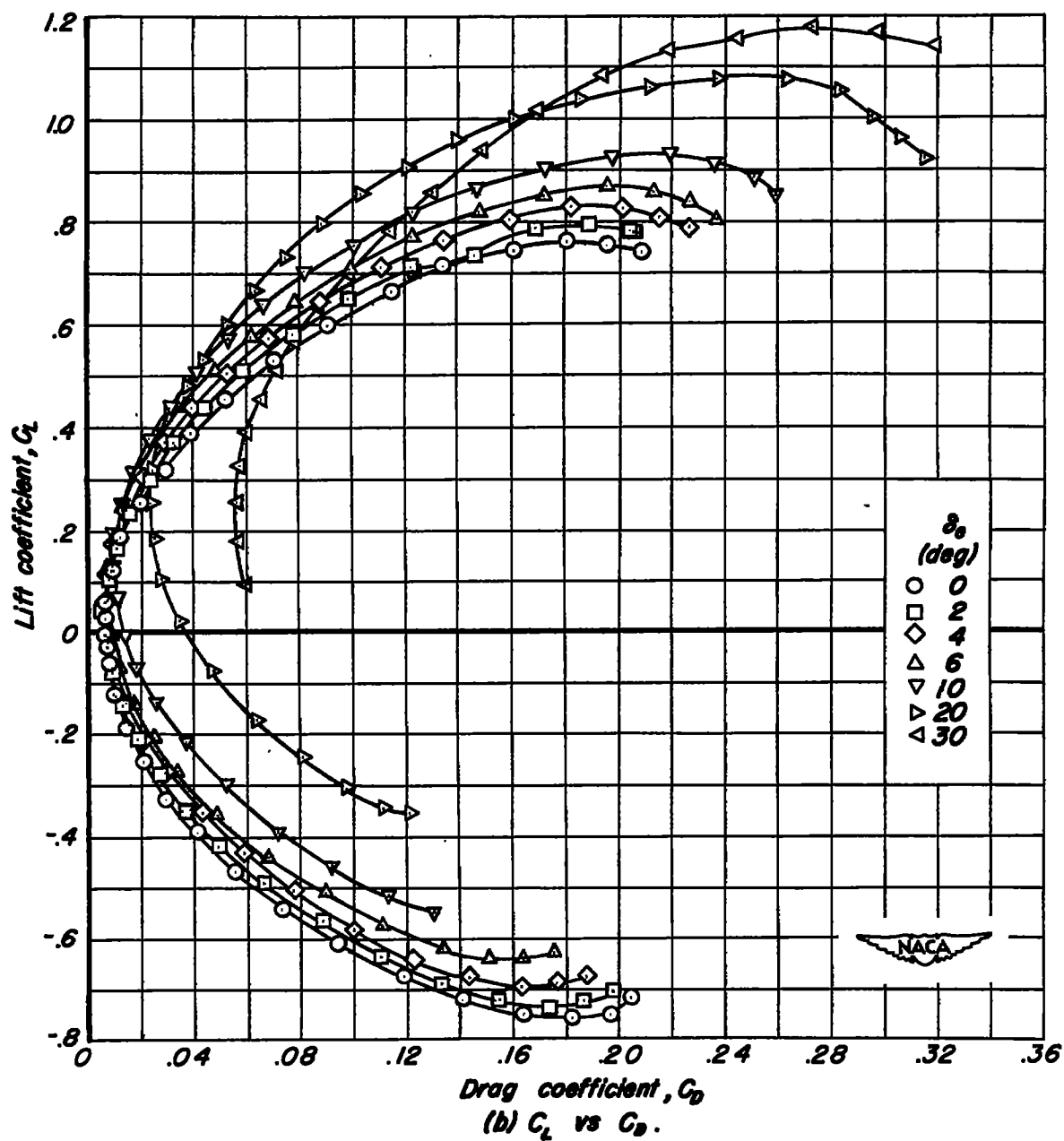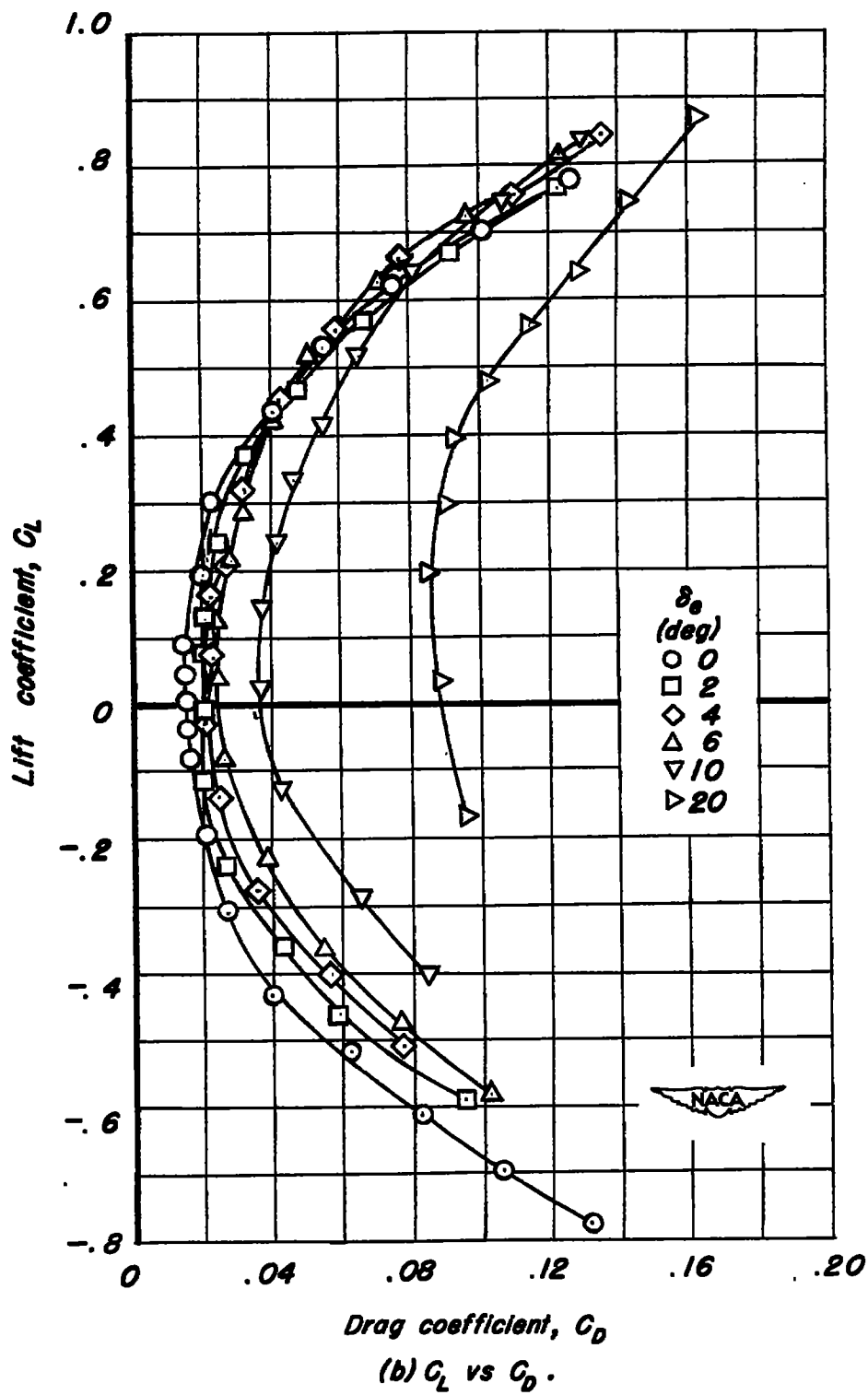
Figure 3. — Concluded.
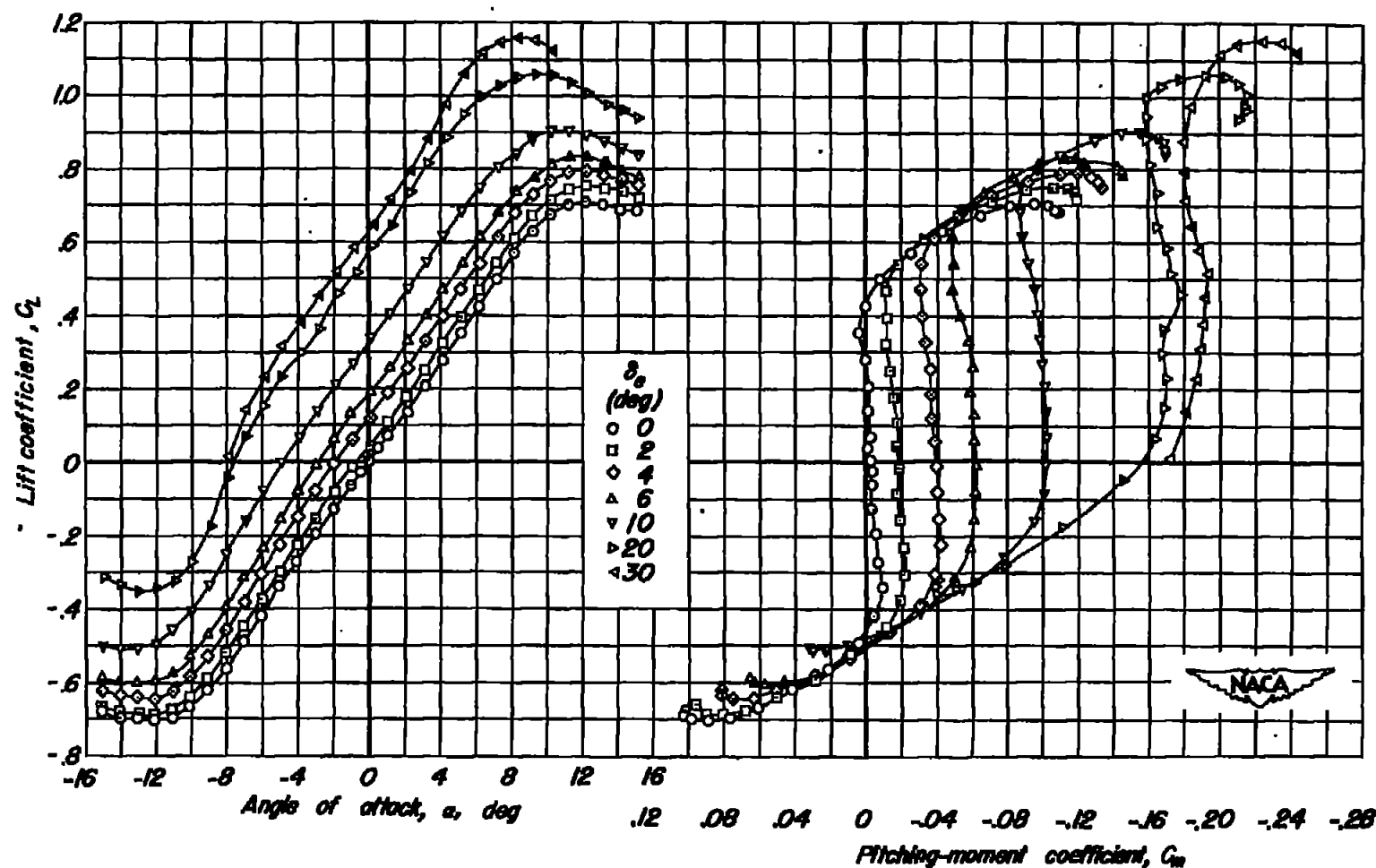
(a) C_L vs α, C_L vs C_m.

Figure 4. — The effect of elevator deflection on the aerodynamic characteristics of the tail at a Mach number of 0.50.

(b) C_L vs C_D.
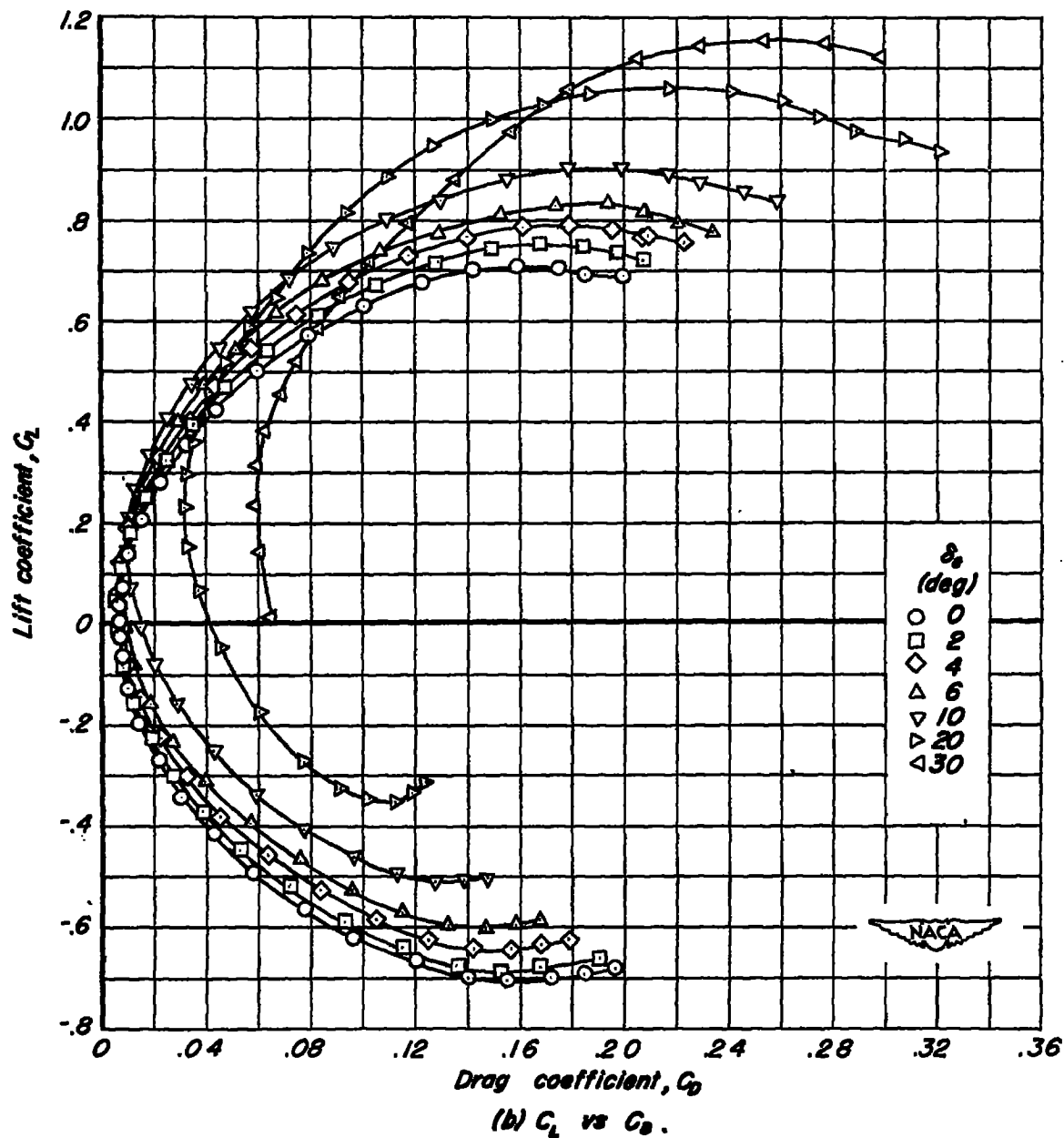
Figure 4. — Concluded.
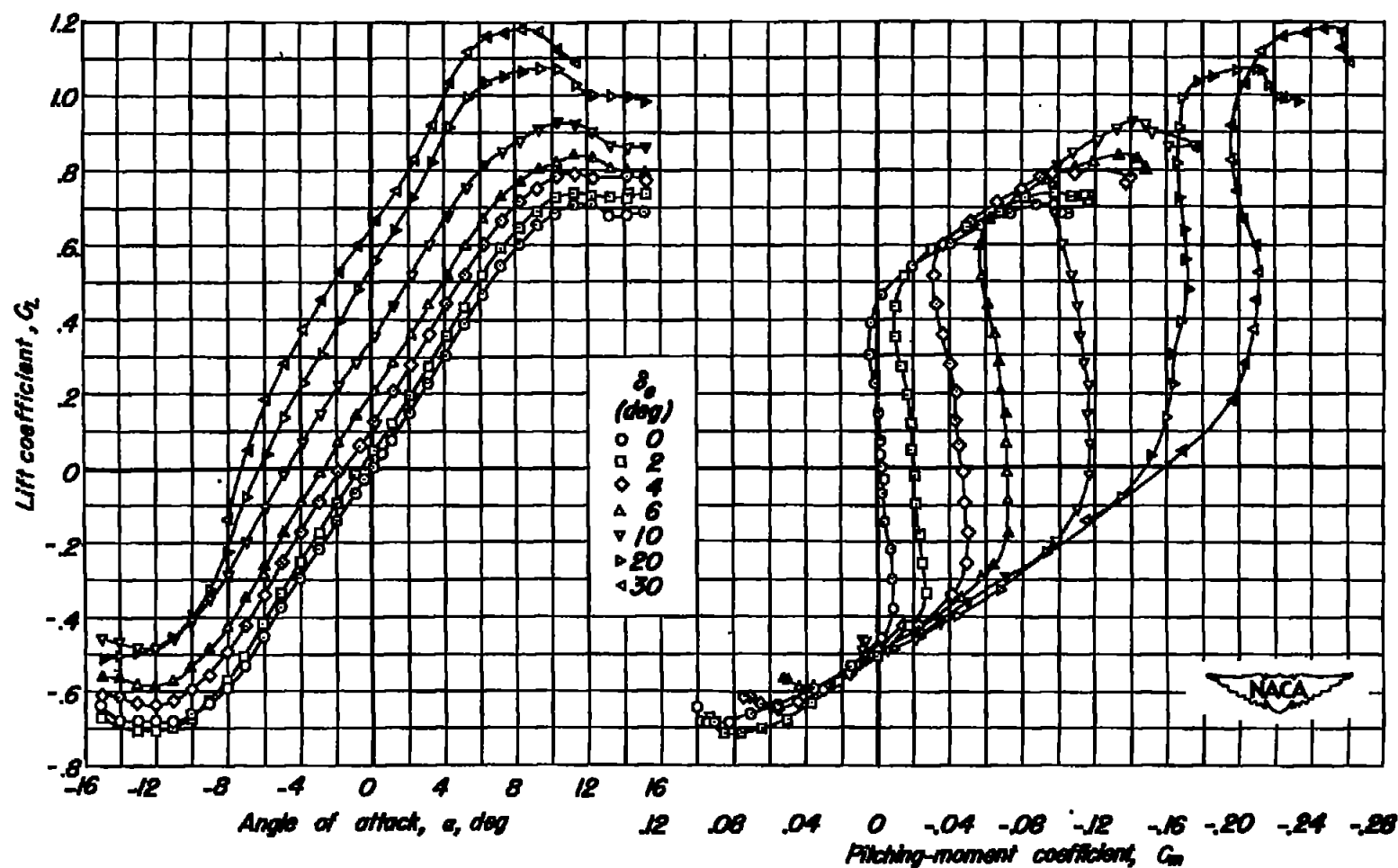
(a) C_L vs α, C_L vs C_m.

Figure 5. — The effect of elevator deflection on the aerodynamic characteristics of the tail at a Mach number of 0.70.

(b) C_L vs C_D.
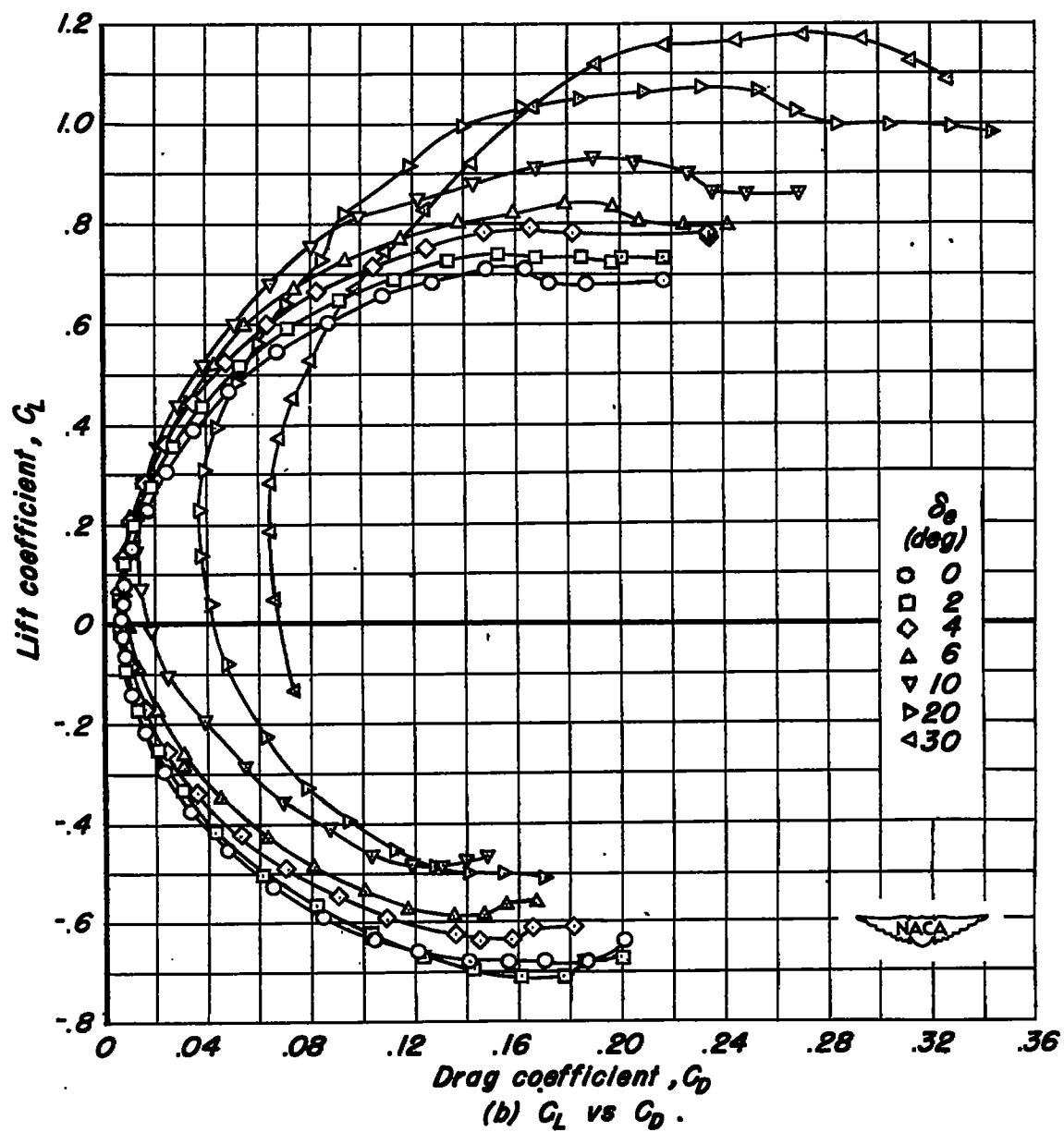
Figure 5.—Concluded.

(a) C_L vs α, C_L vs C_m.
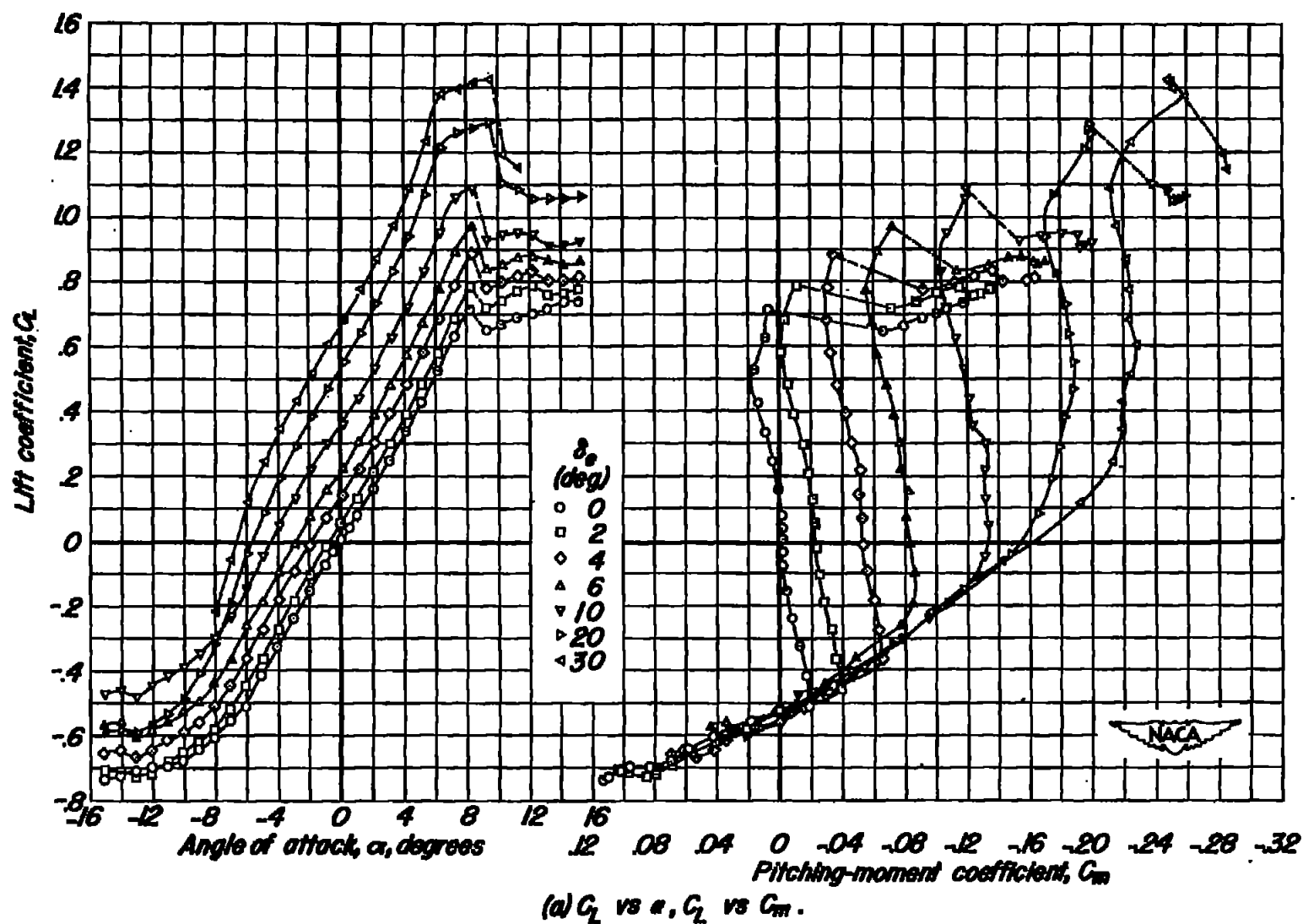
Figure 6. — The effect of elevator deflection on the aerodynamic characteristics of the tail at a Mach number of 0.80.
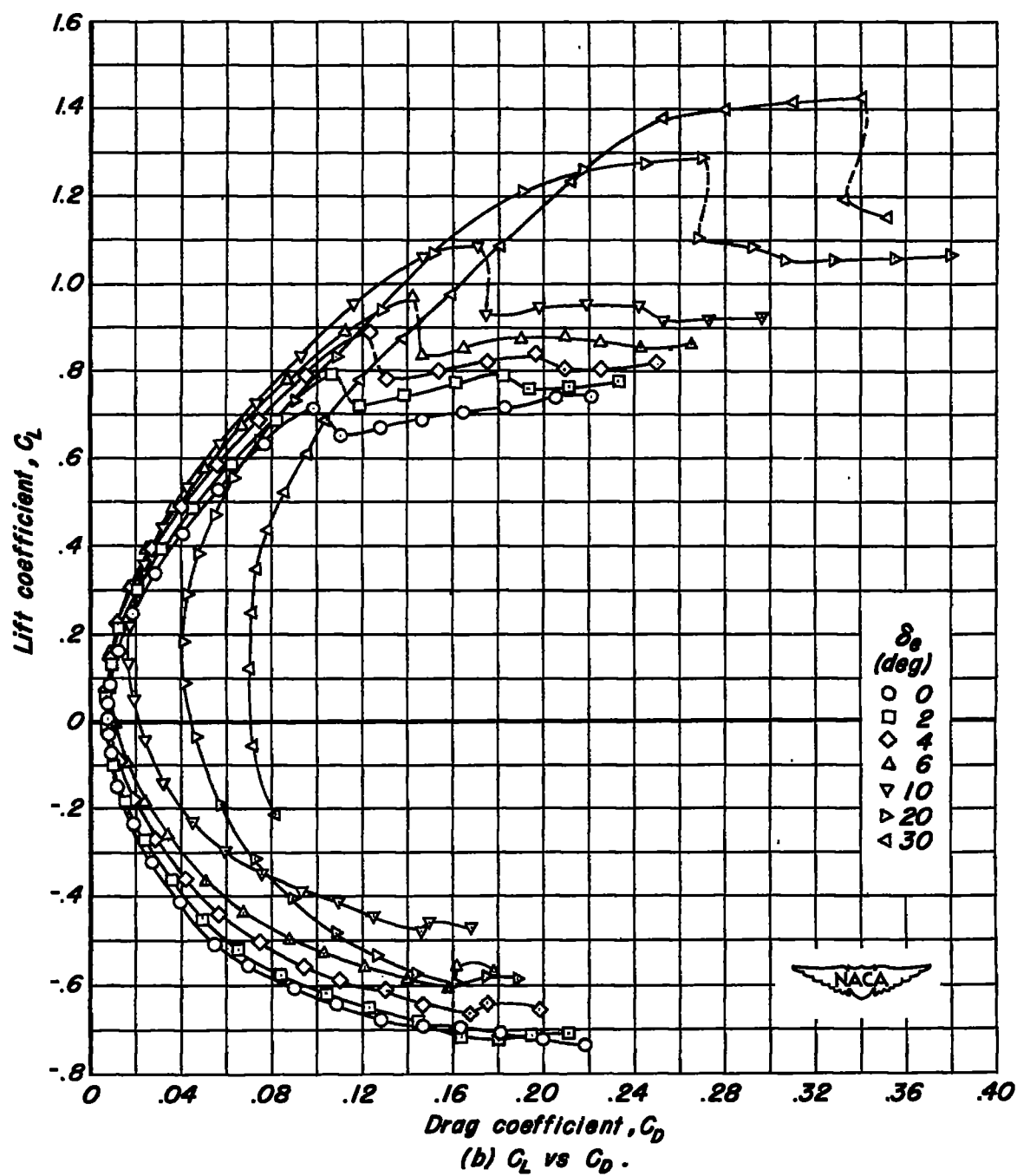
Figure 6.—Concluded.

(b) C_L vs C_D.
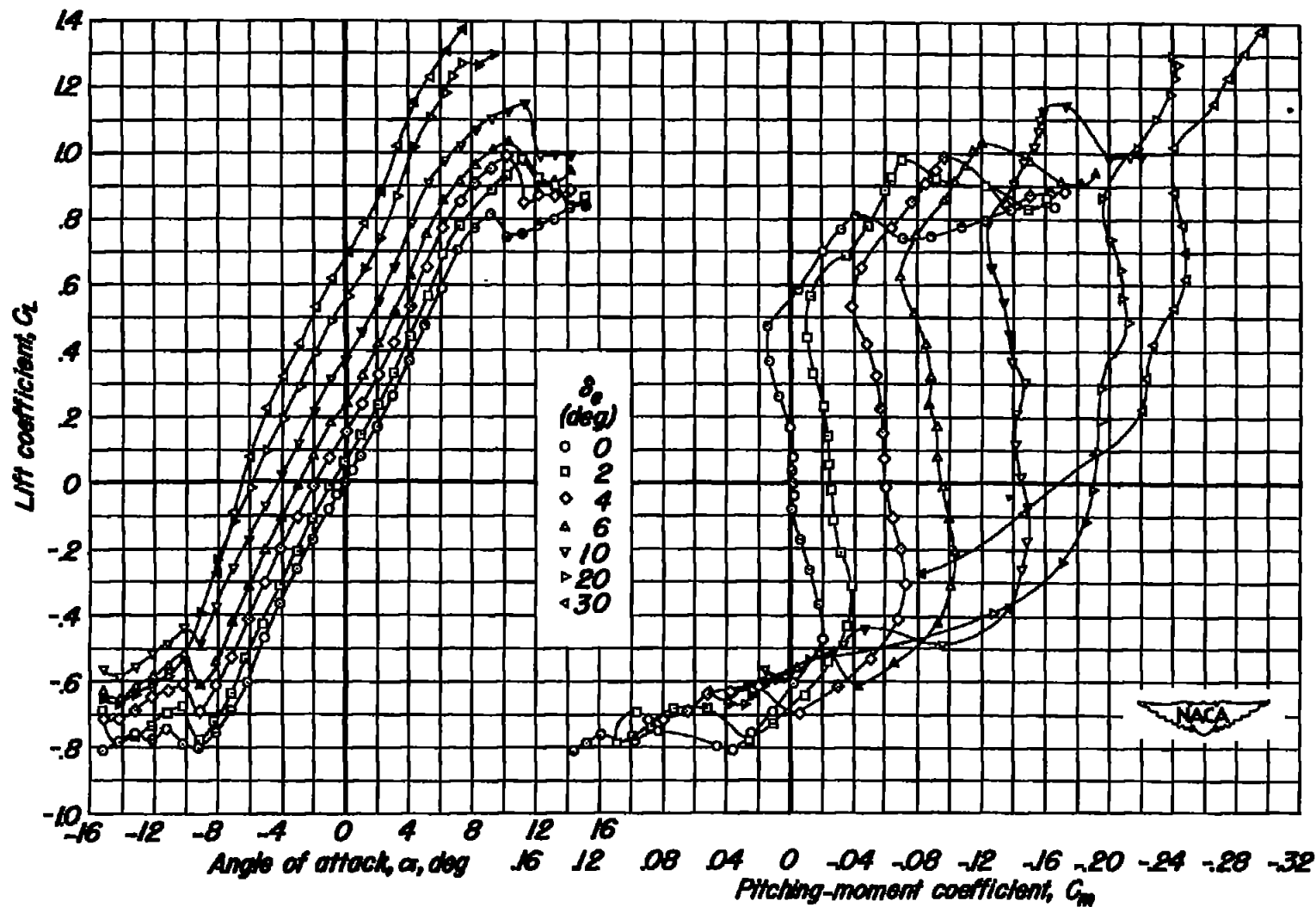
(a) C_L vs α, C_L vs C_m.

Figure 7. — The effect of elevator deflection on the aerodynamic characteristics of the tail at a Mach number of 0.85.

(b) C_L vs C_D.
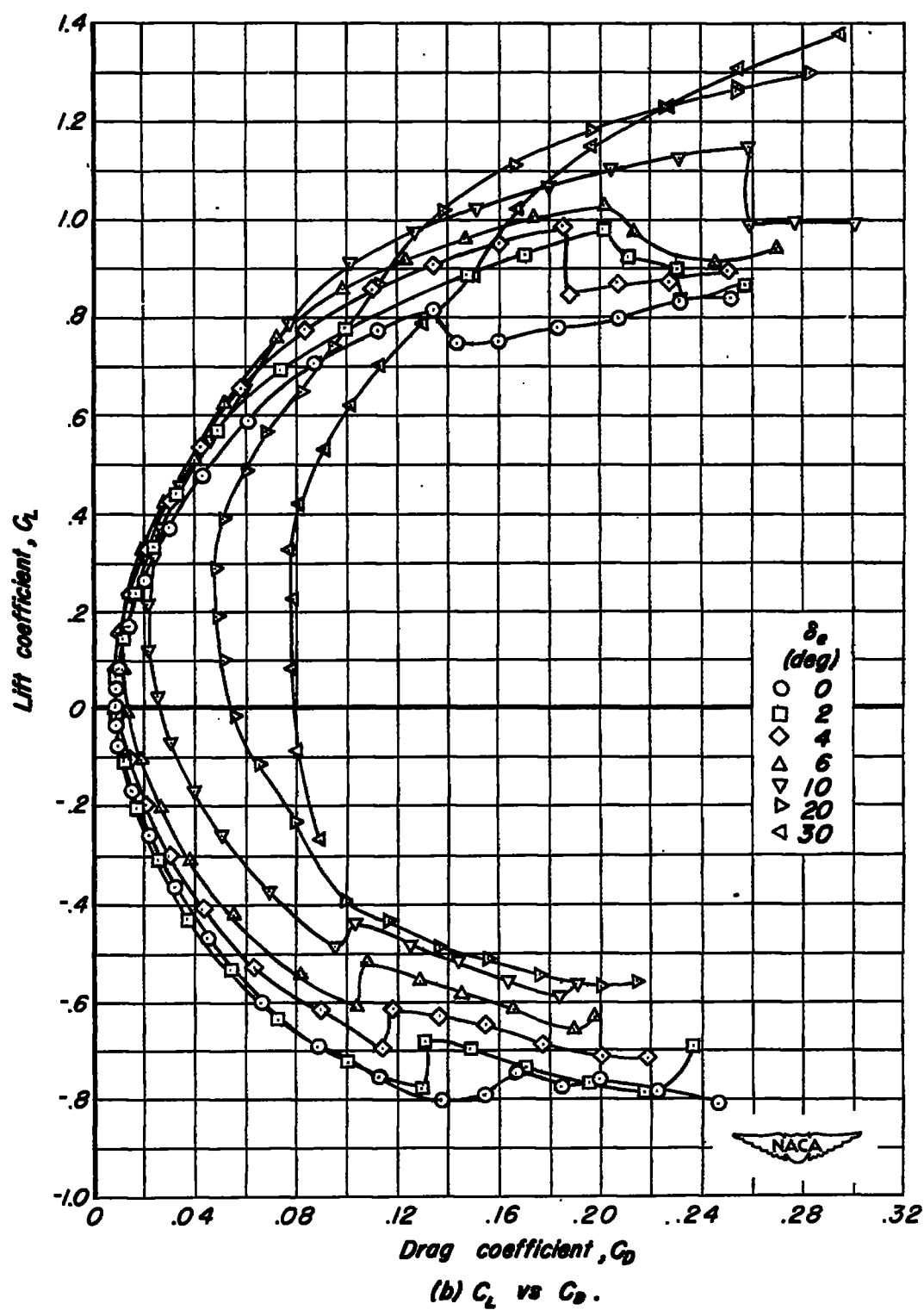
Figure 7. — Concluded.

δ_e
(deg)
○ 0
□ 2
◇ 4
△ 6
▽ 10
▷ 20
◁ 30

Lift coefficient, C_L

Angle of attack, α, deg

Pitching-moment coefficient, C_m
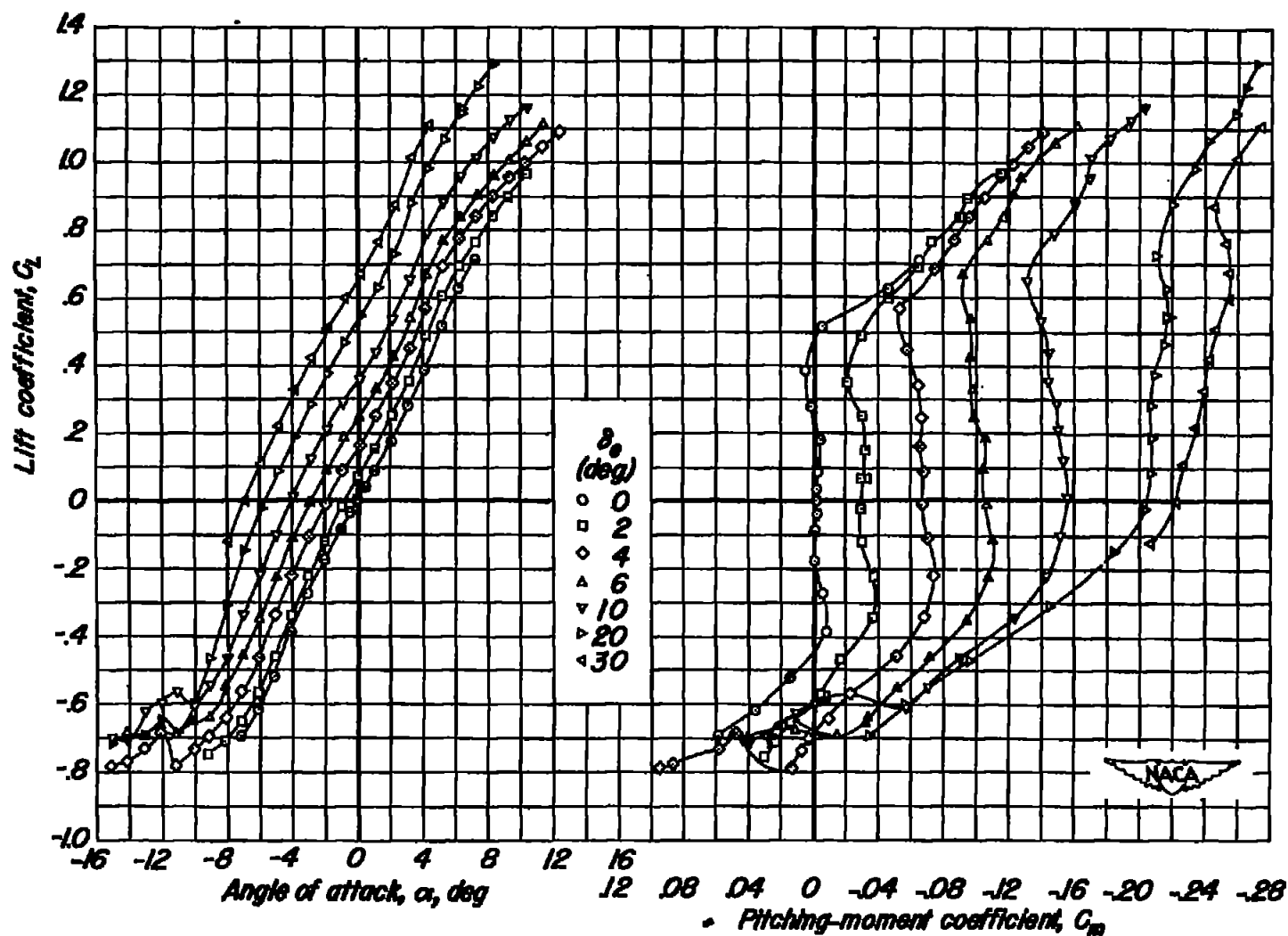
(a) C_L vs α, C_L vs C_m.

Figure 8. — The effect of elevator deflection on the aerodynamic characteristics of the tail at a Mach number of 0.87.

(b) C_L vs C_D.
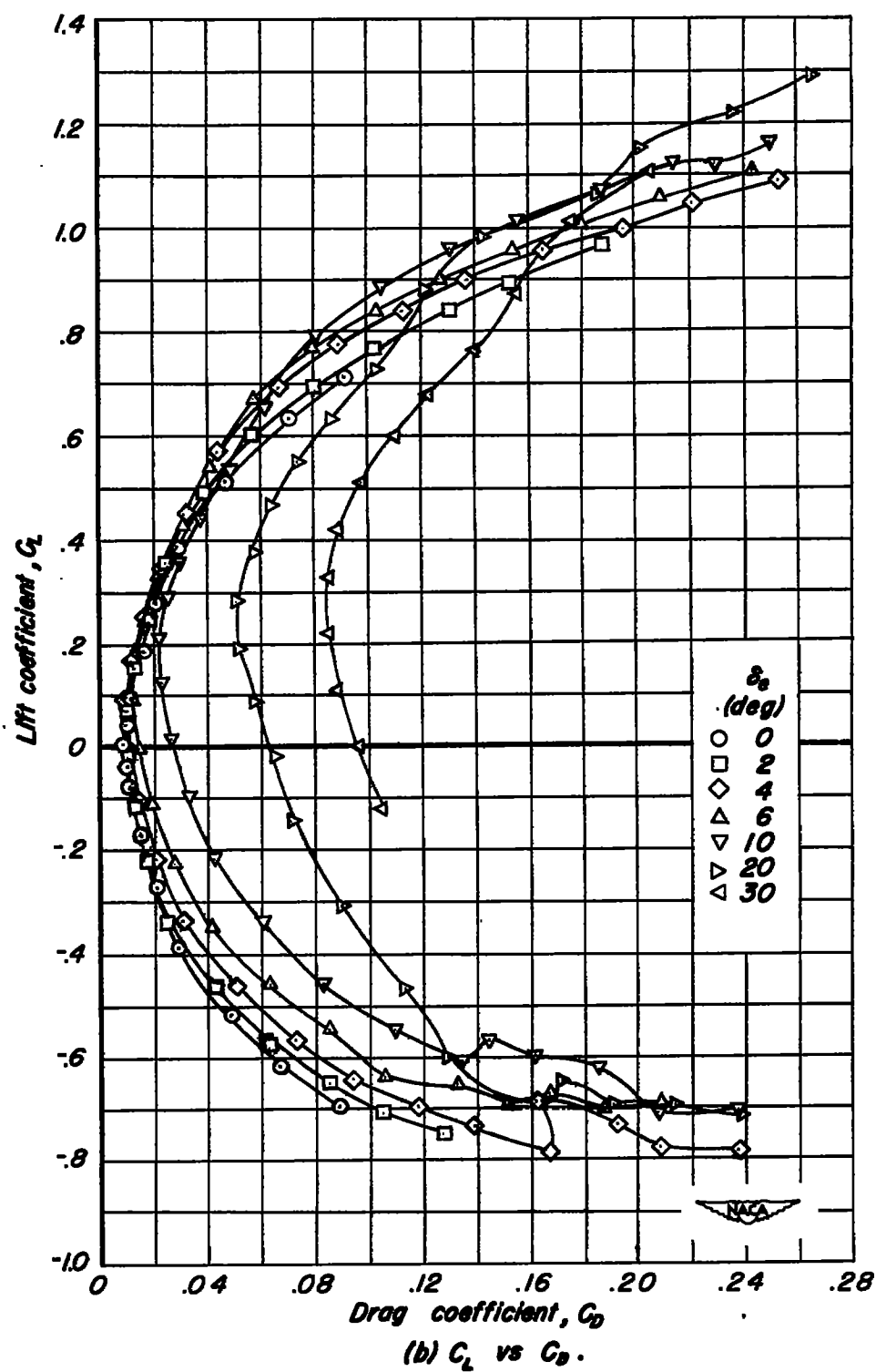
Figure 8. — Concluded.
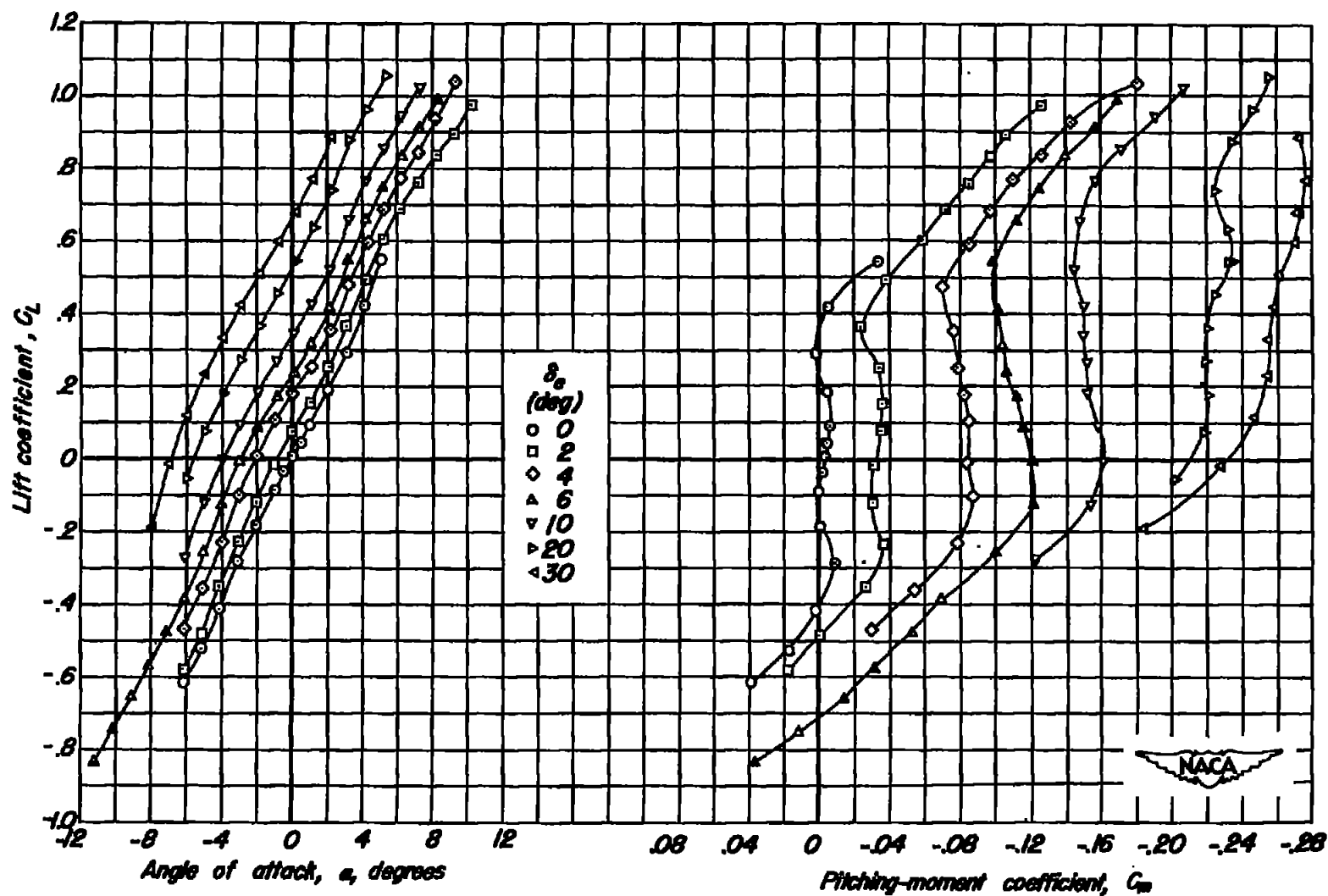
(a) C_L vs α, C_L vs C_m.

Figure 9. — The effect of elevator deflection on the aerodynamic characteristics of the tail at a Mach number of 0.90.

(b) C_L vs C_D.
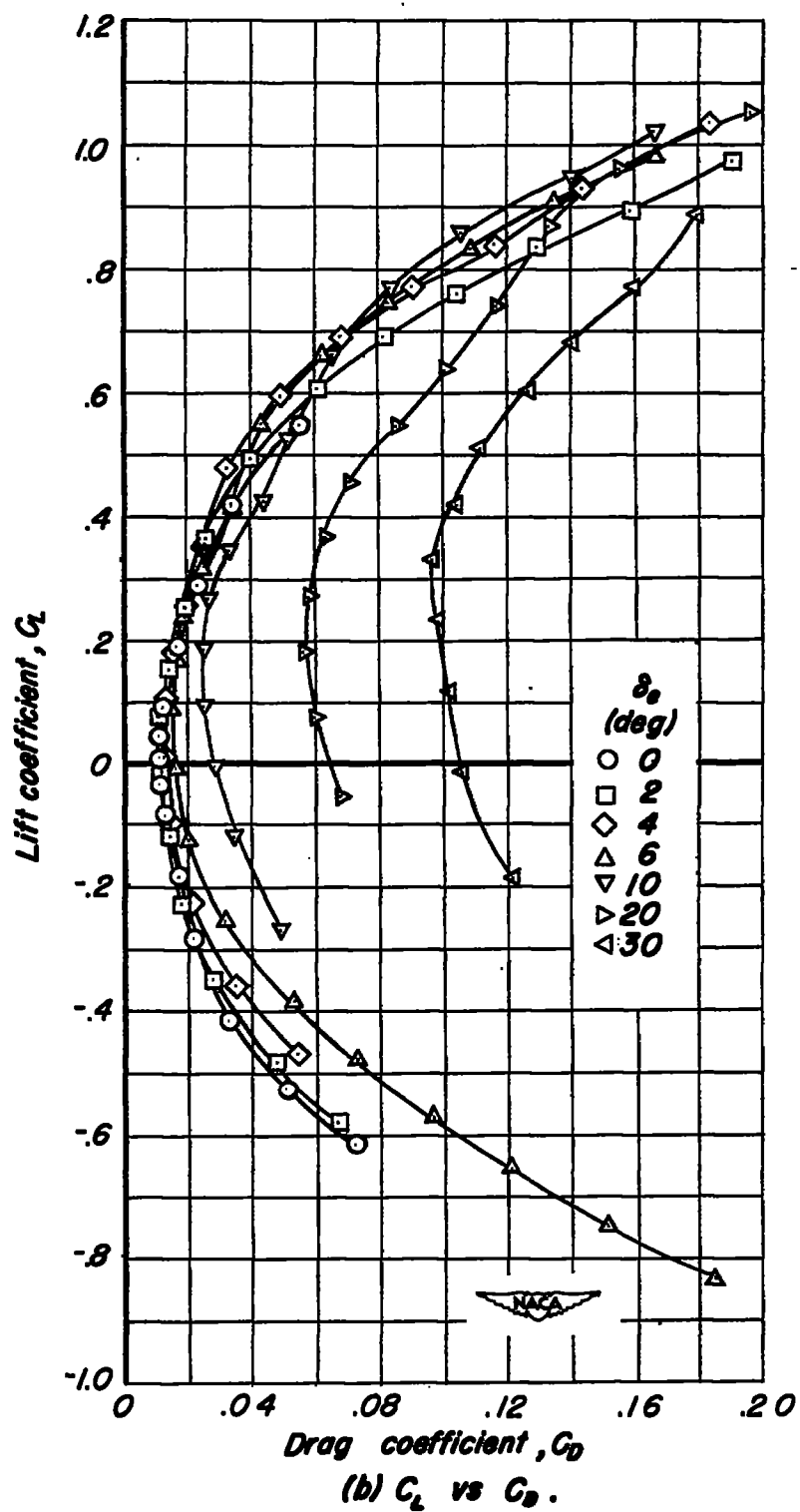
Figure 9. — Concluded.

(a) C_L vs α , C_L vs C_m .
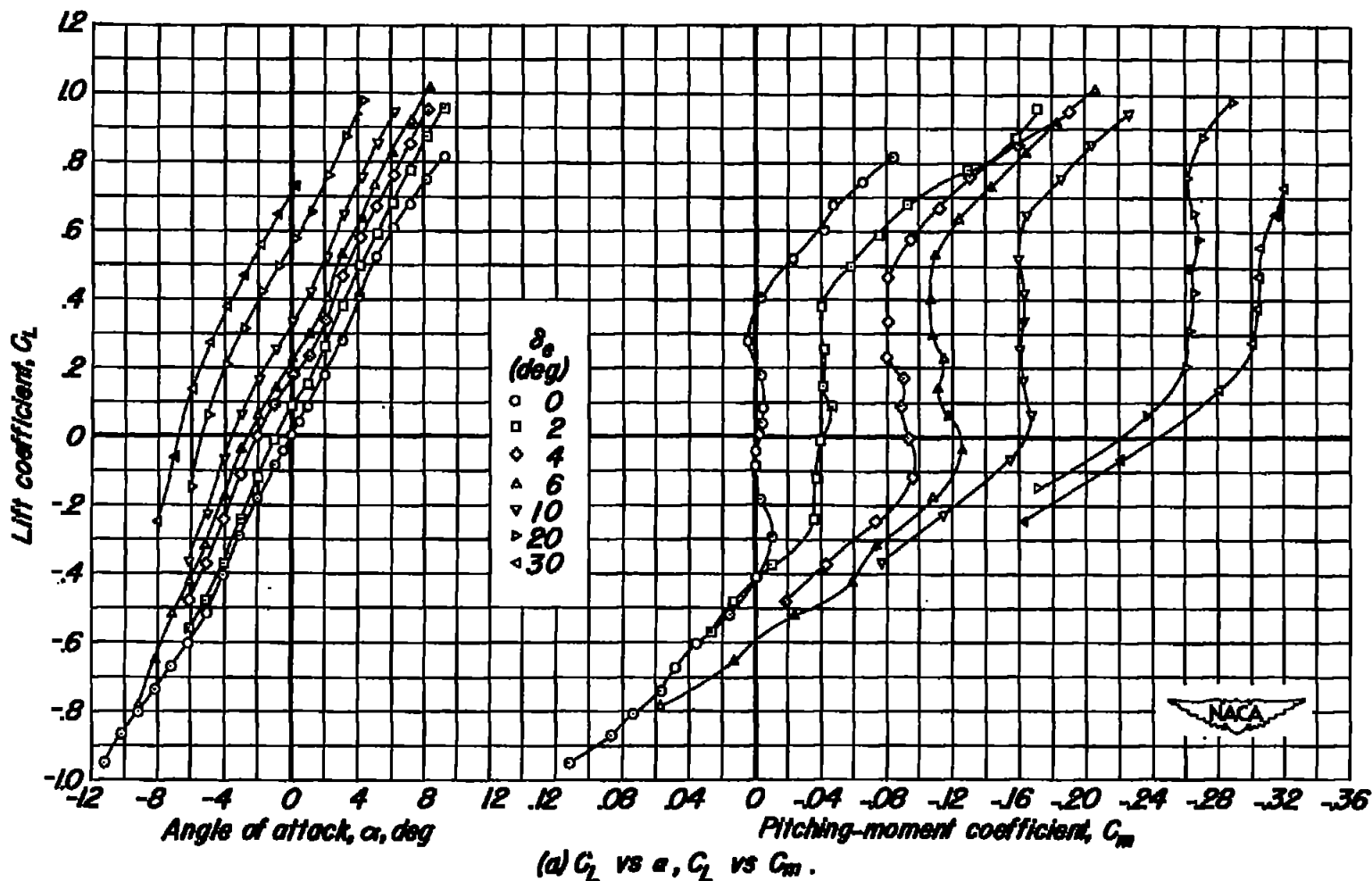
Figure 10.—— The effect of elevator deflection on the aerodynamic characteristics of the tail at a Mach number of 0.92.

(b) C_L vs C_D.

Figure 10. — Concluded.

(a) C_L vs α, C_L vs C_m.

Figure 11.— The effect of elevator deflection on the aerodynamic characteristics of the tail at a Mach number of 0.94.

(b) C_L vs C_D.

Figure II.— Concluded.

Elevator deflection, δ_e , deg
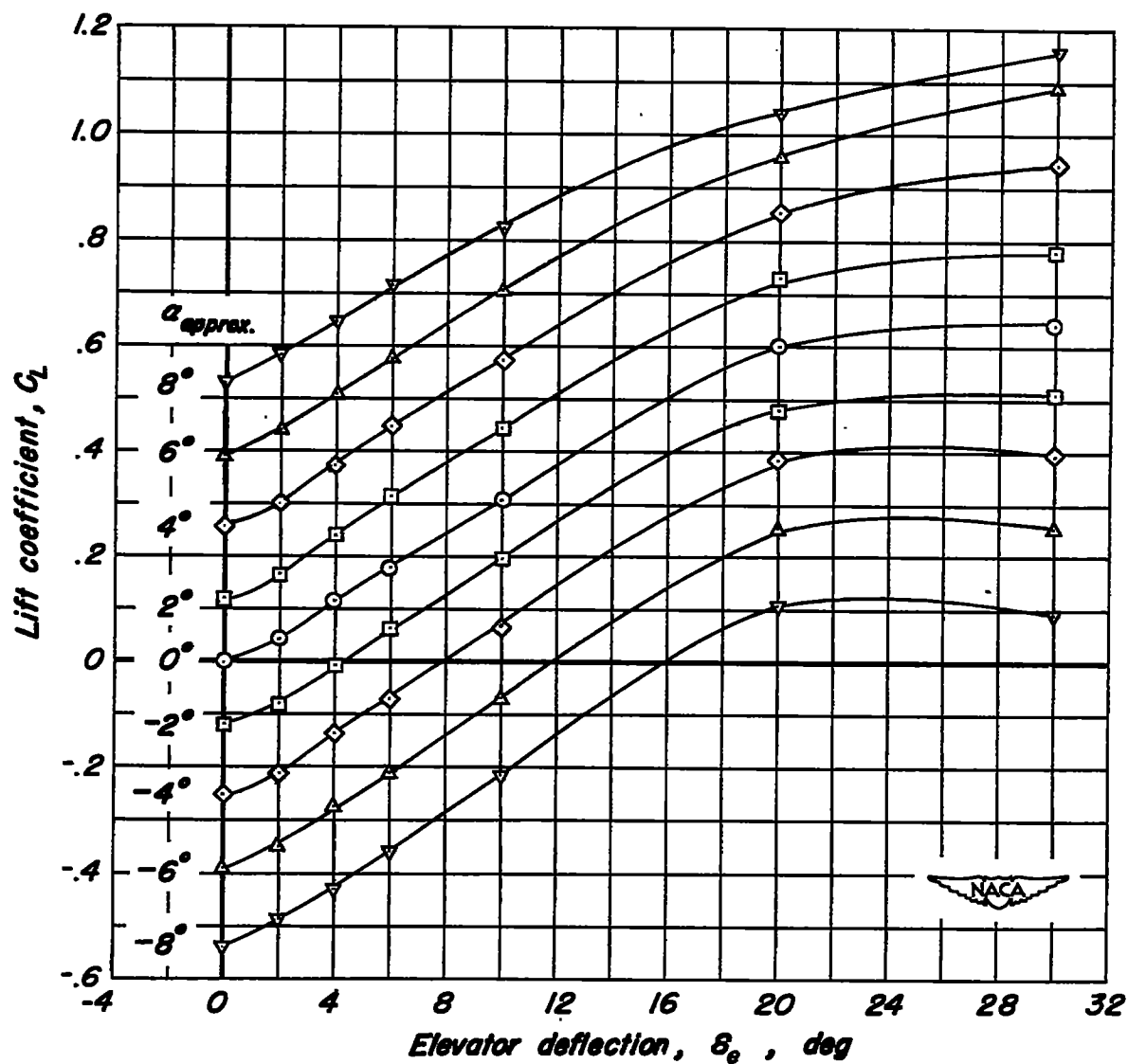
(a) M, 0.20 .

Figure 12.——The variation of lift coefficient with elevator deflection for various angles of attack of the tail .

Figure 12. — Continued .

(b) M, 0.50.

Elevator deflection, δ_e , deg

(c) M, 0.70.
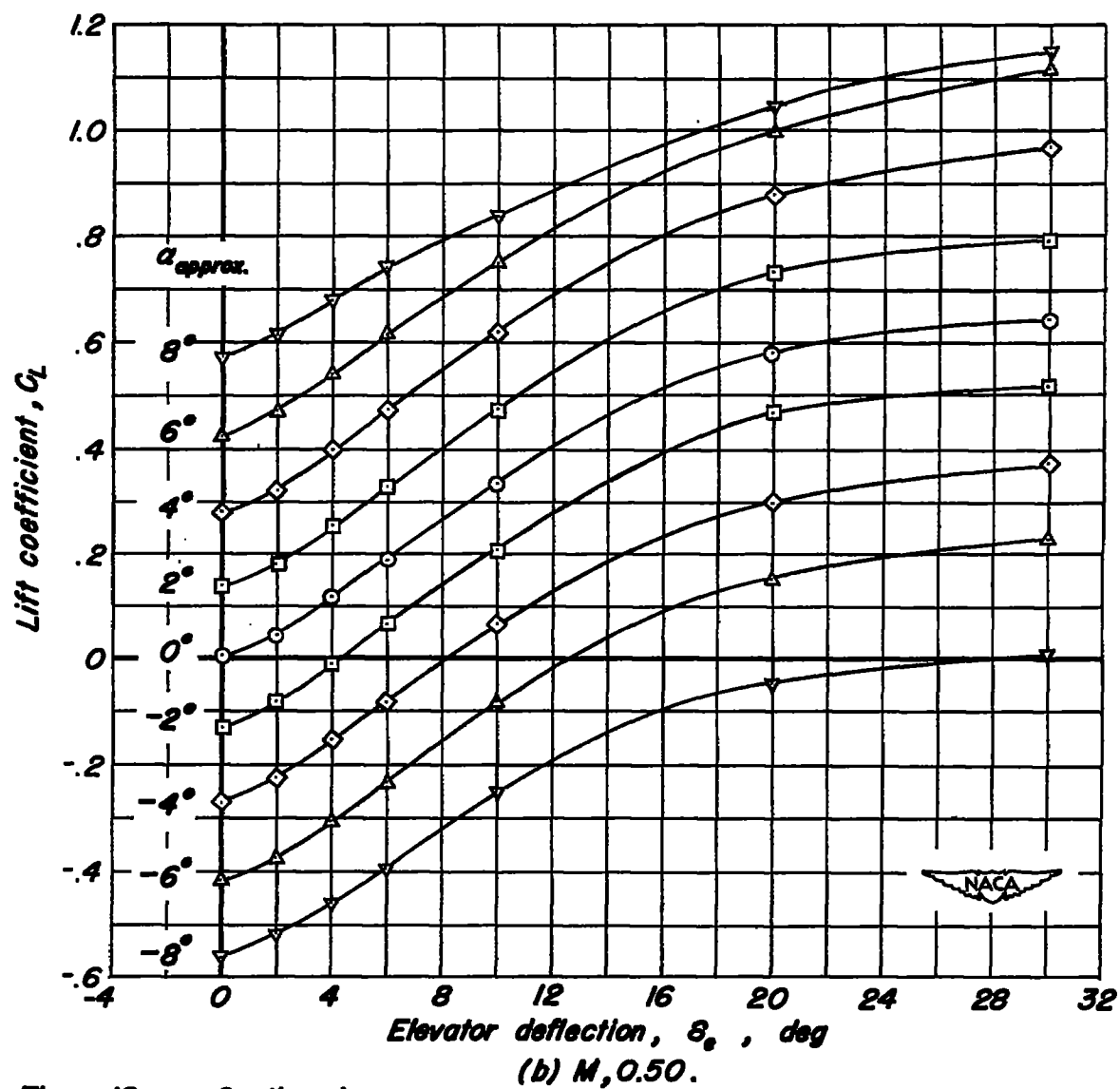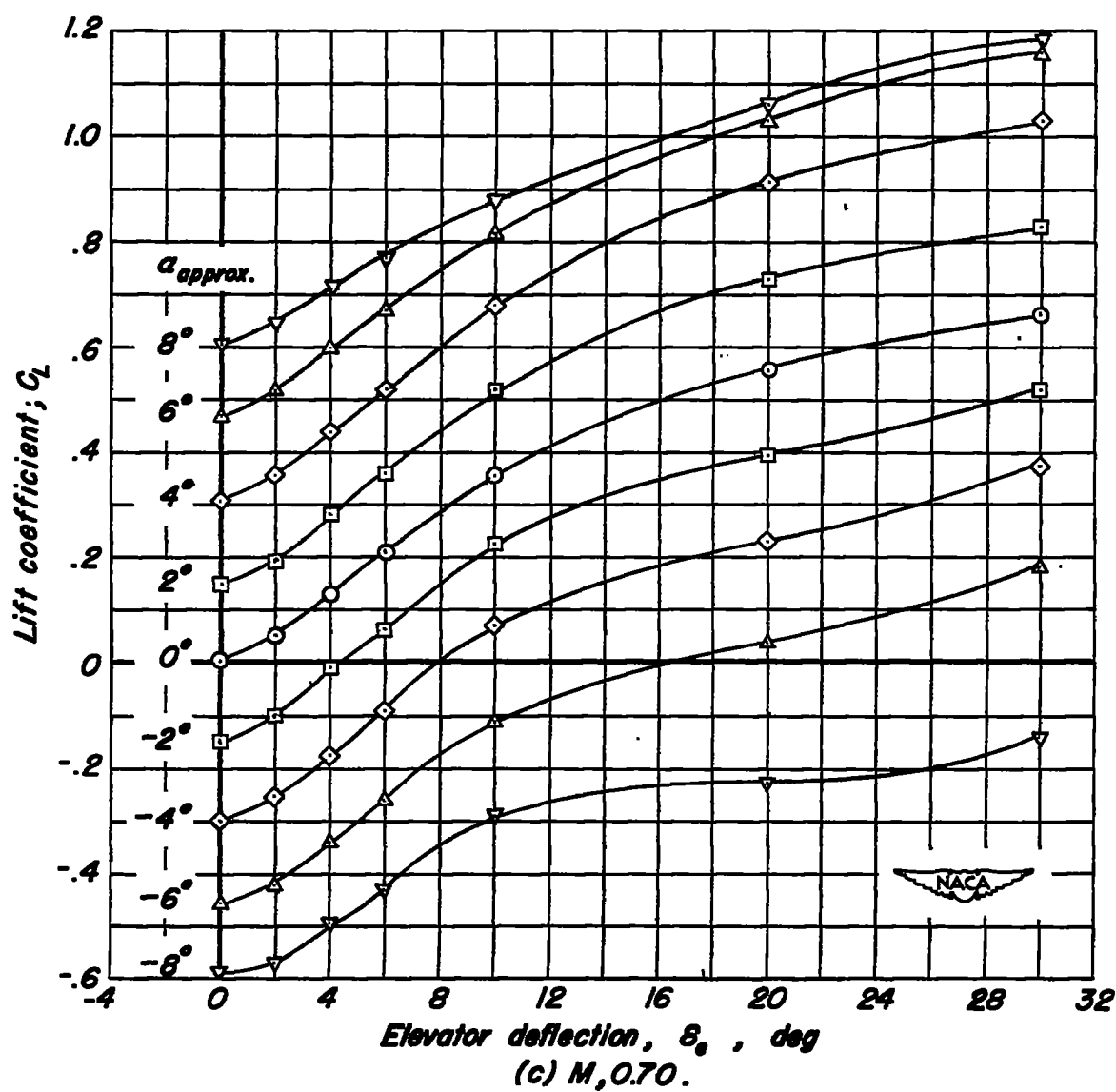
Figure 12. — Continued .

Figure 12. — Continued .
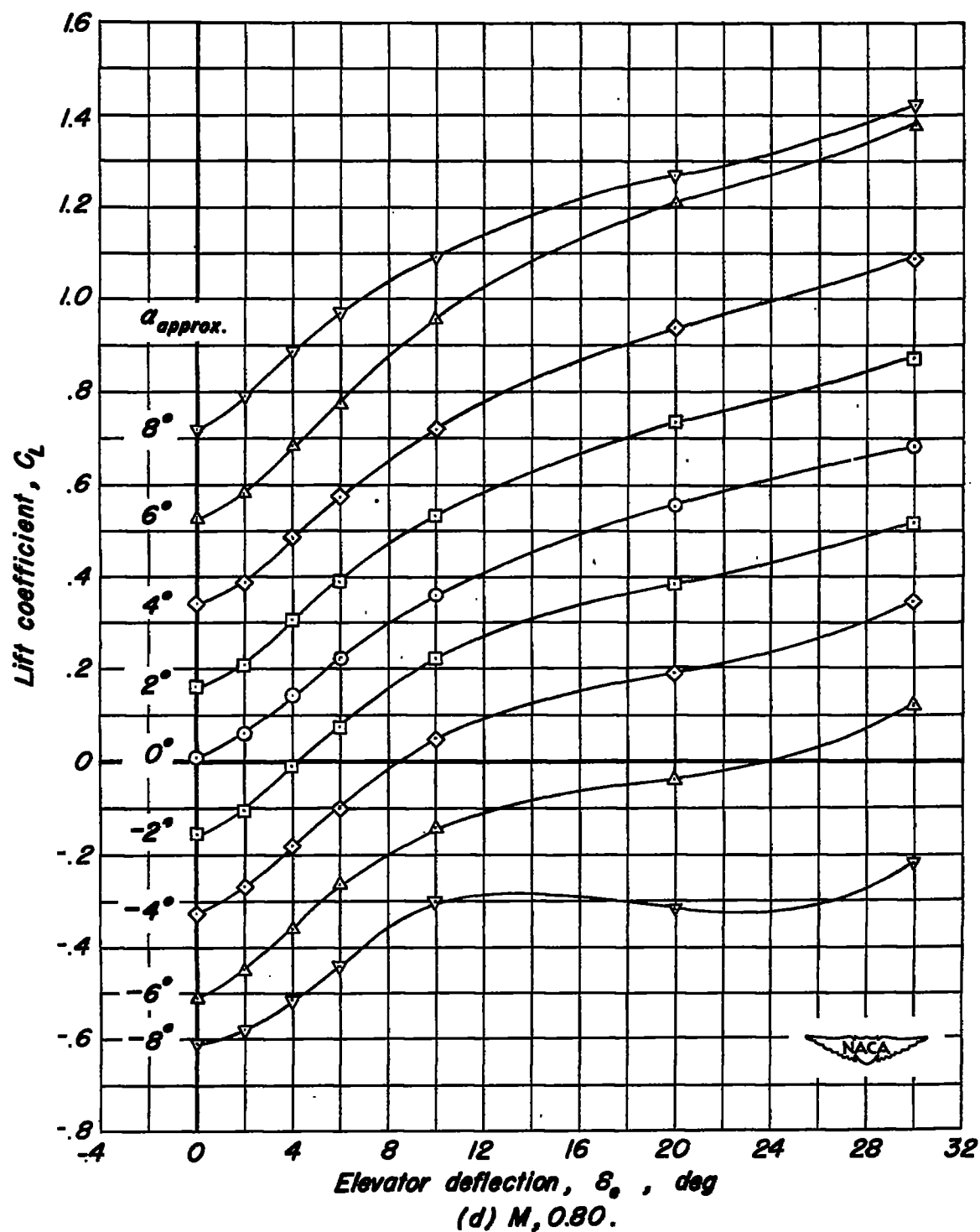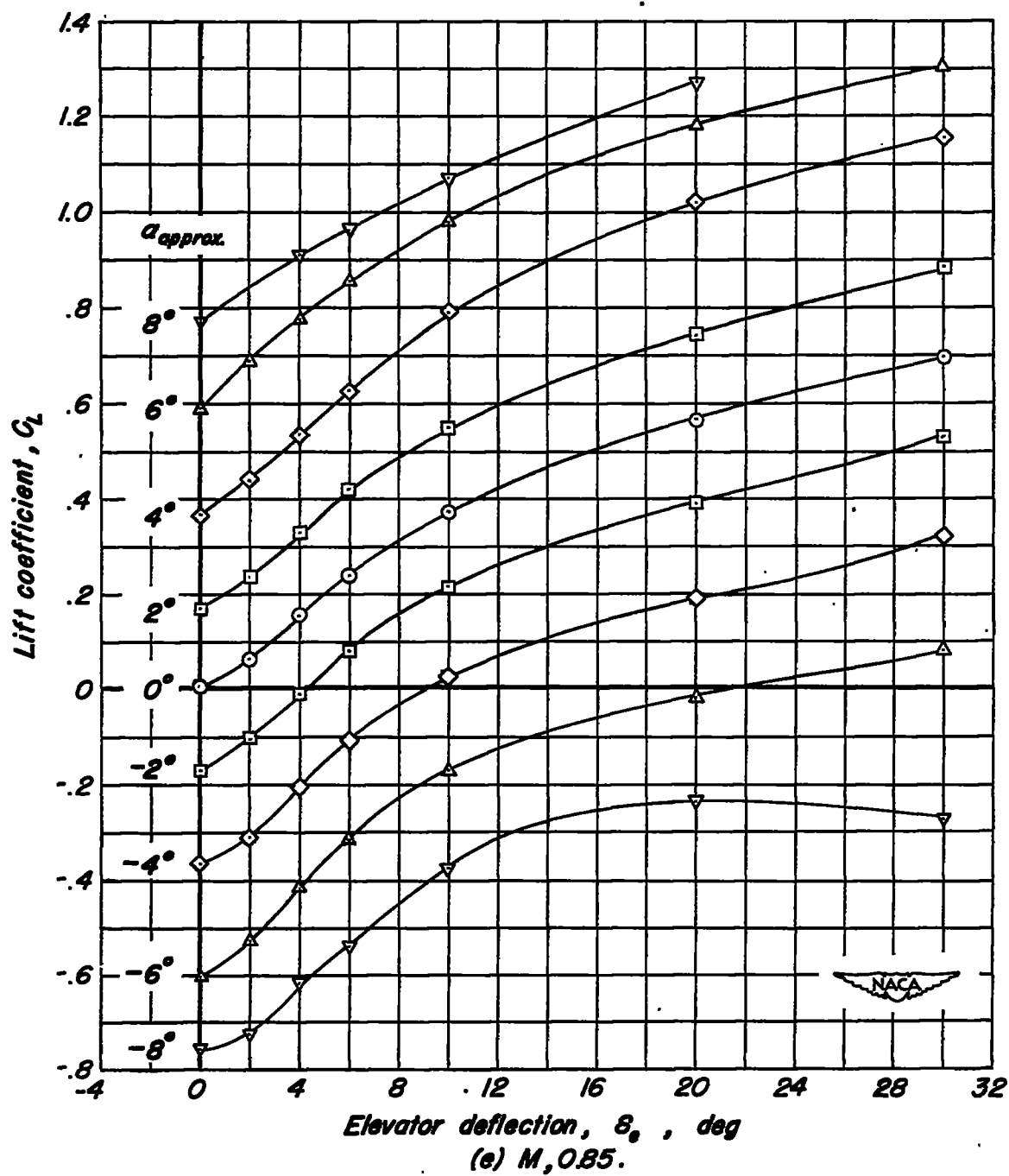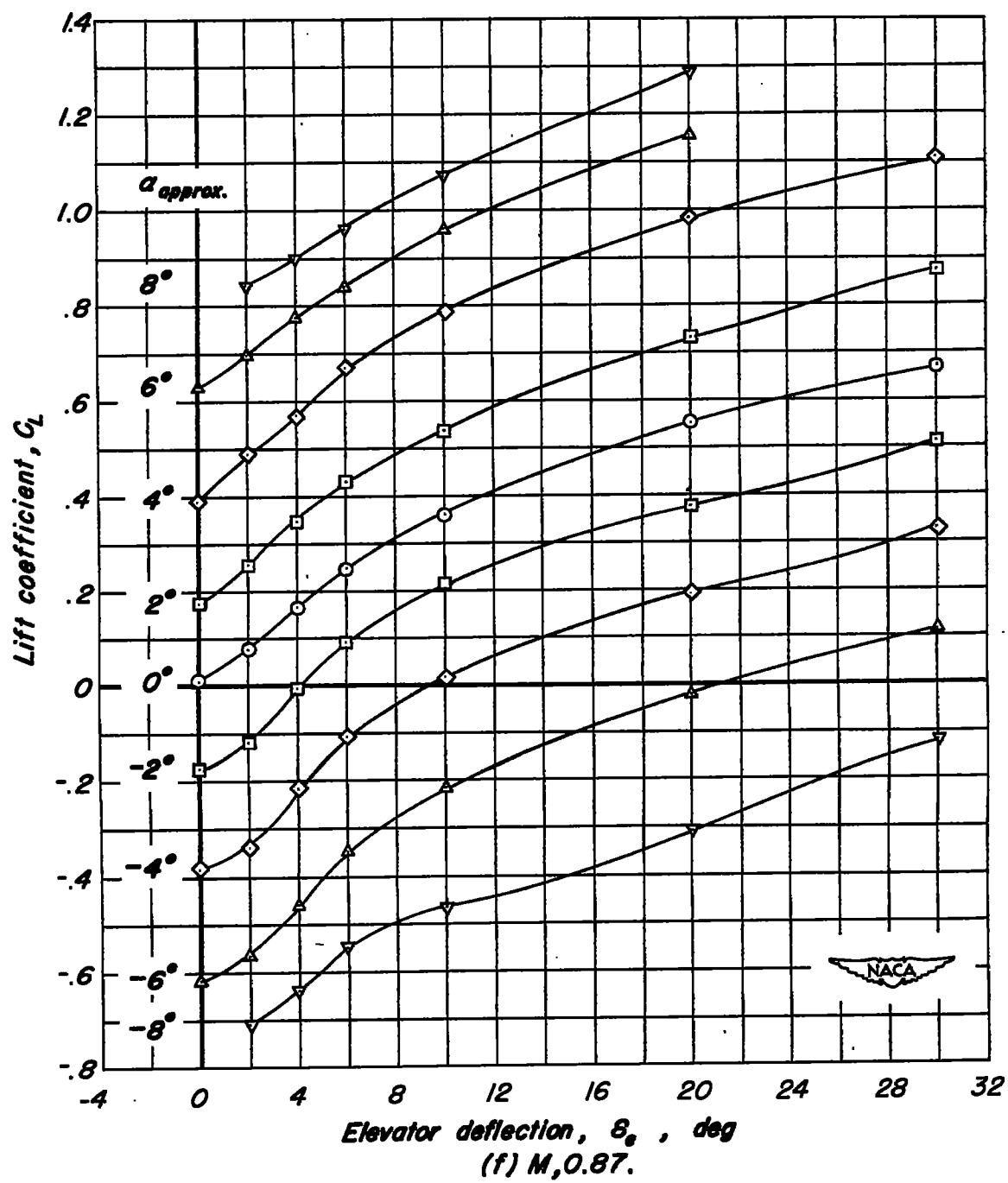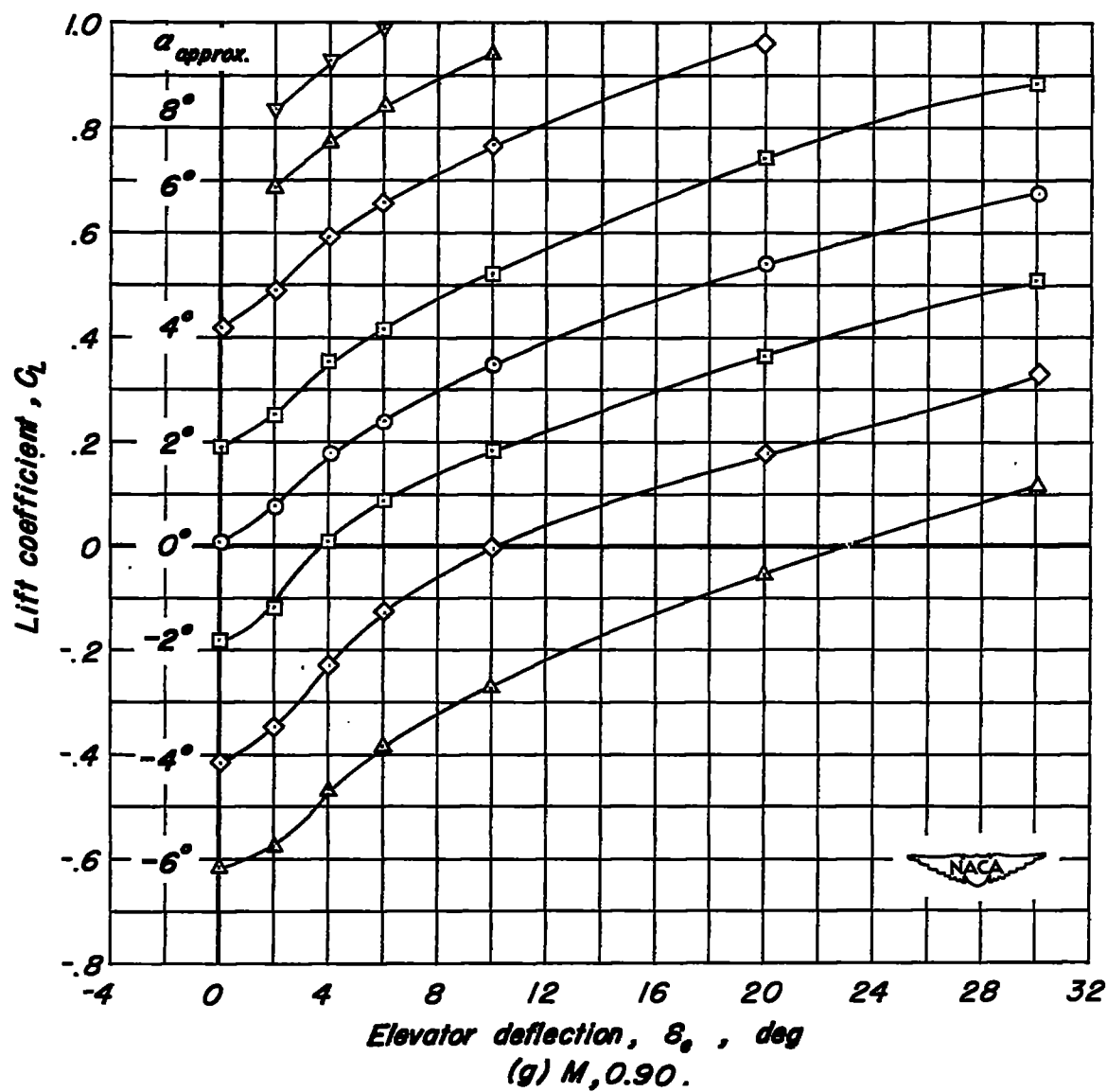
(d) M, 0.80.

Elevator deflection, δ_e , deg

Lift coefficient, C_L

Figure 12. — Continued.

(e) M, 0.85.

Elevator deflection, δ_e, deg

Elevator deflection, δ_e , deg

(f) M, 0.87.

Figure 12. — Continued .

Elevator deflection, δ_e , deg

(g) M, 0.90.

Figure 12. — Continued .

(h) M, 0.92.
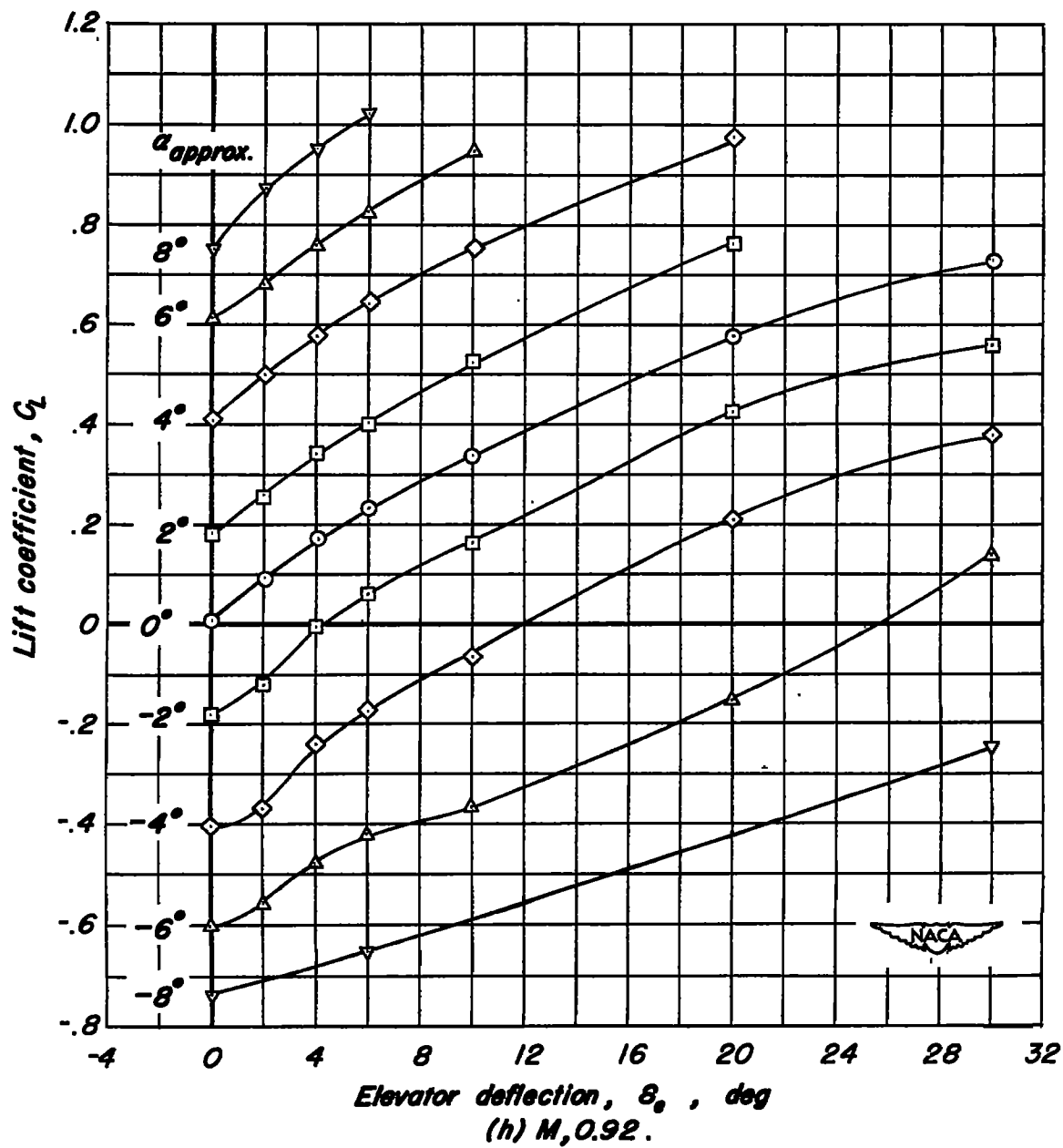
Figure 12. — Continued.
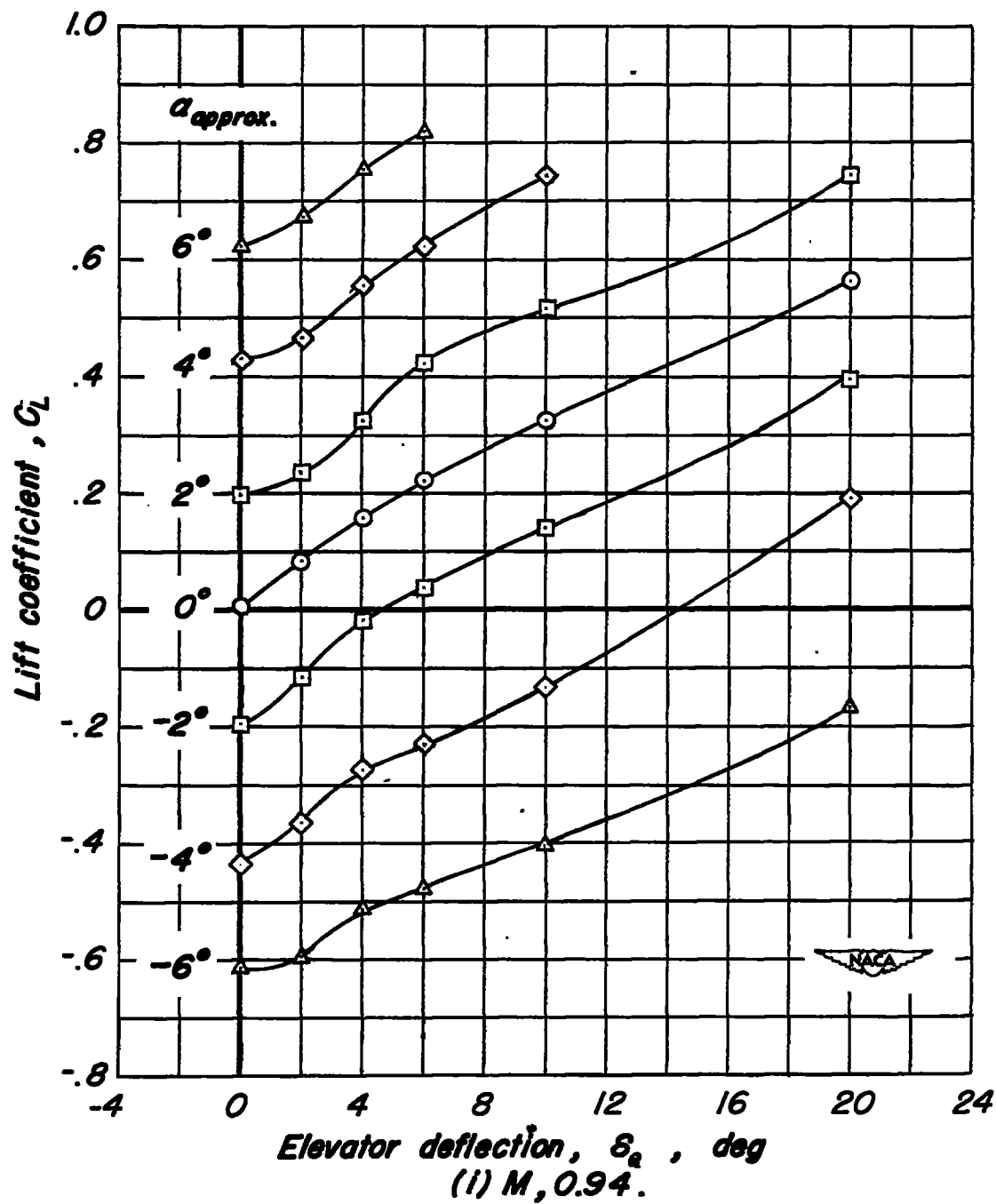
Figure 12.— Concluded .

(a) δ_e, 0°.
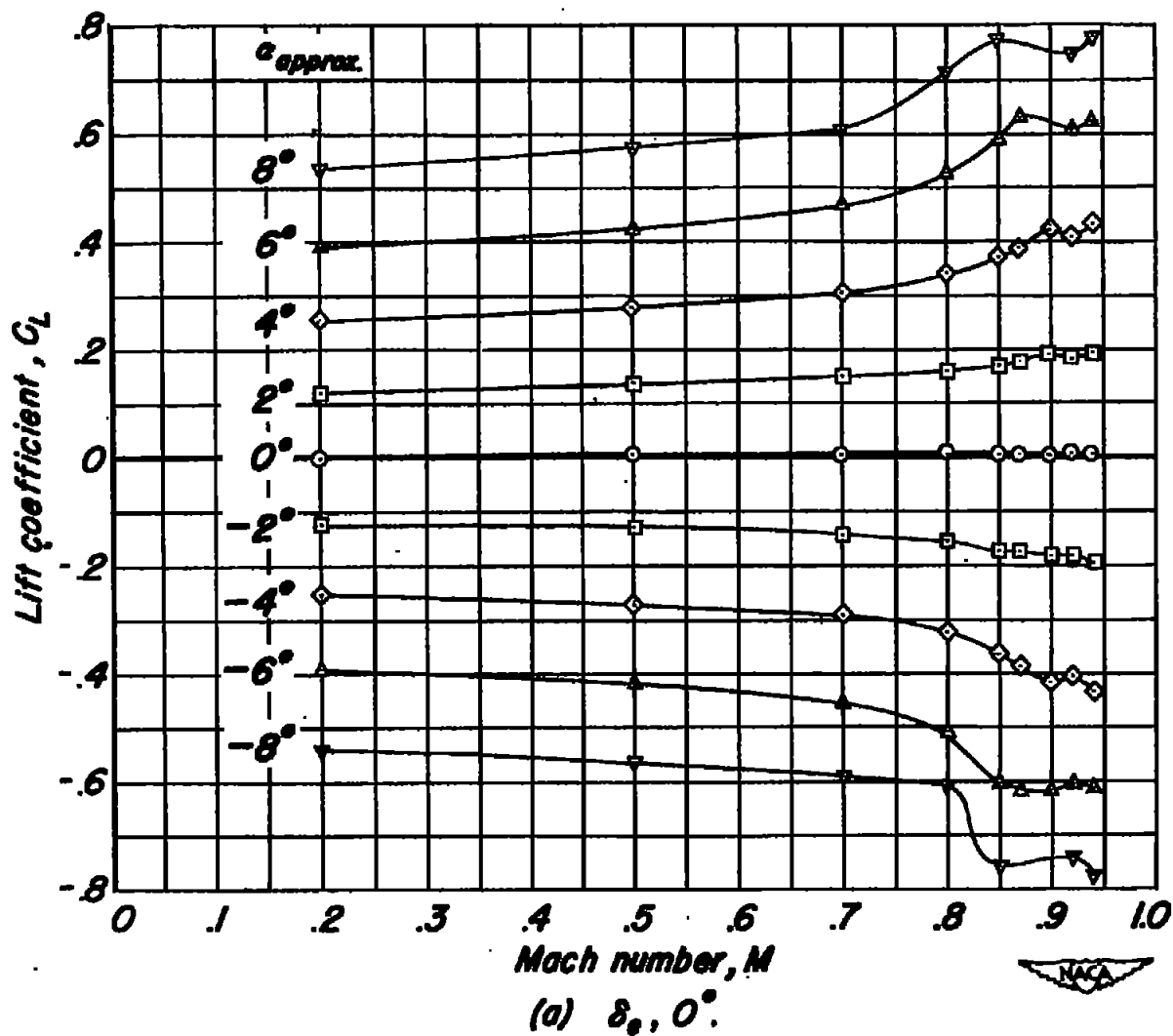
Figure 13.— The variation of lift coefficient with Mach number for various angles of attack of the tail.

(b) δ_e, 4°.

Figure 13.— Continued.

(c) δ_e, 10°.

Figure 13.— Continued .

(d) δ_e , $20°$.

Figure 13.— Continued .

(e) δ_e , 30°.
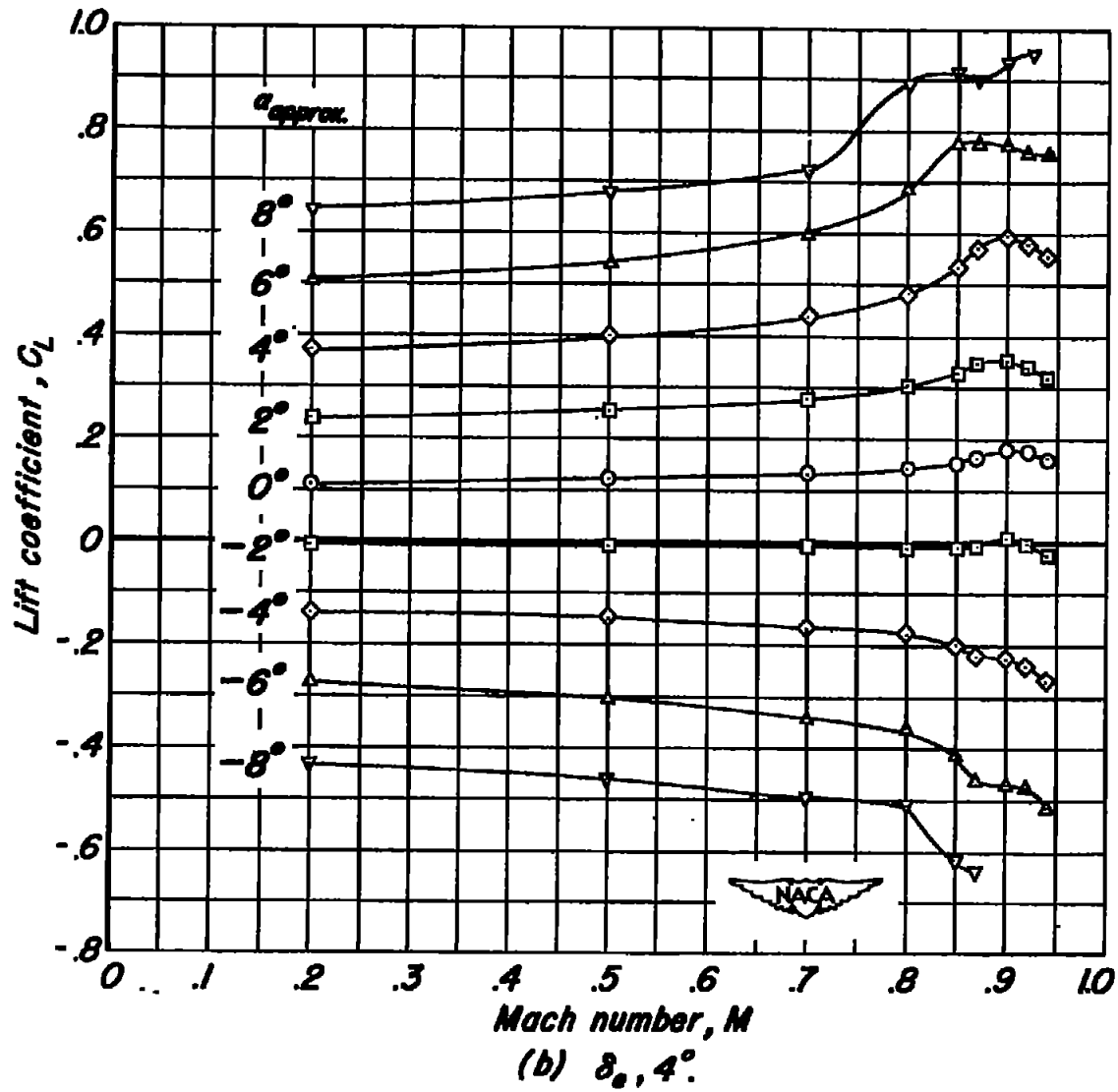
Figure 13.— Concluded.
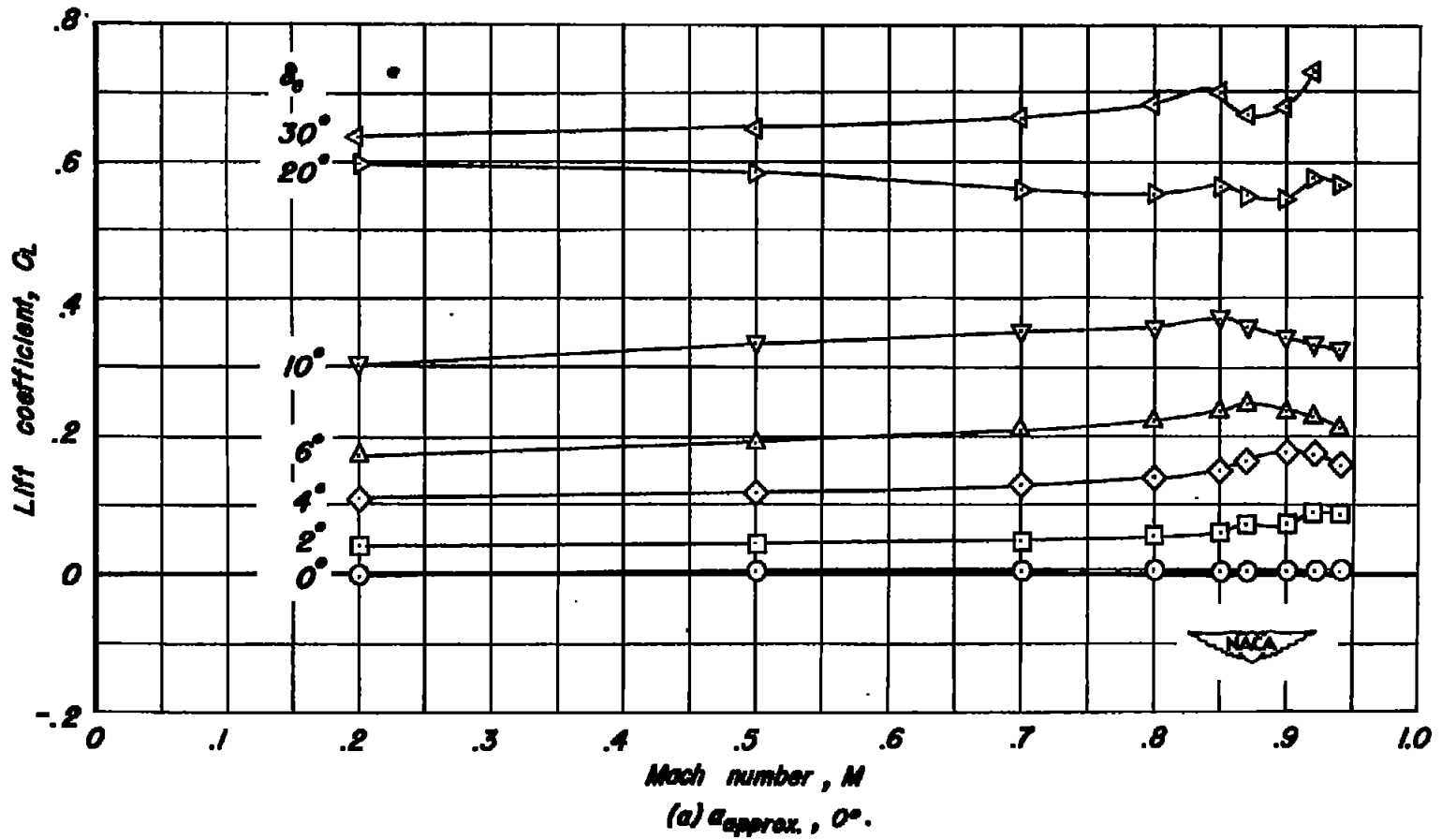
Figure 14.—The variation of lift coefficient with Mach number for various elevator deflections.

(a) $a_{approx.}$, $0°$.

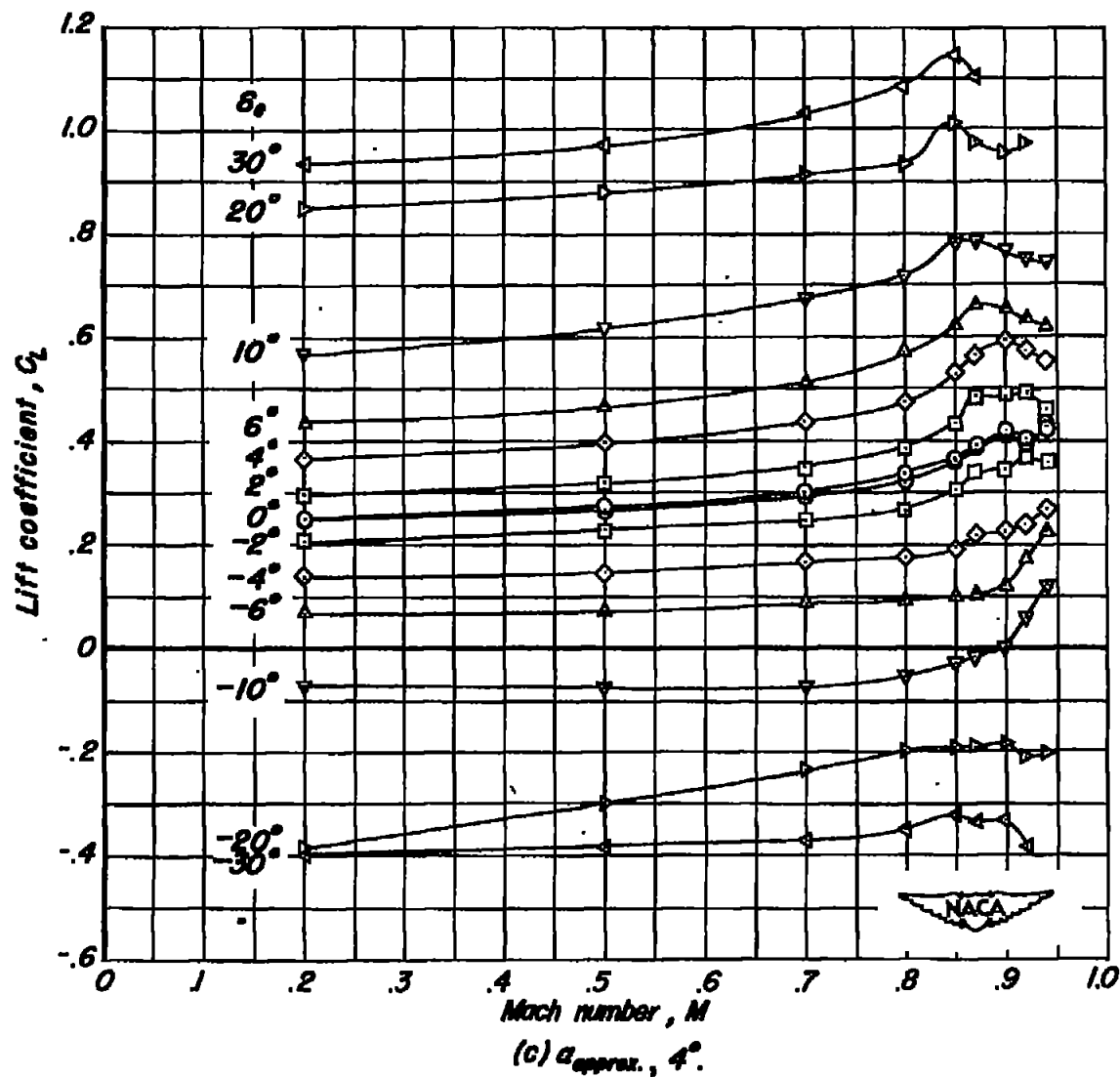(b) $a_{approx.}$, $2°$.
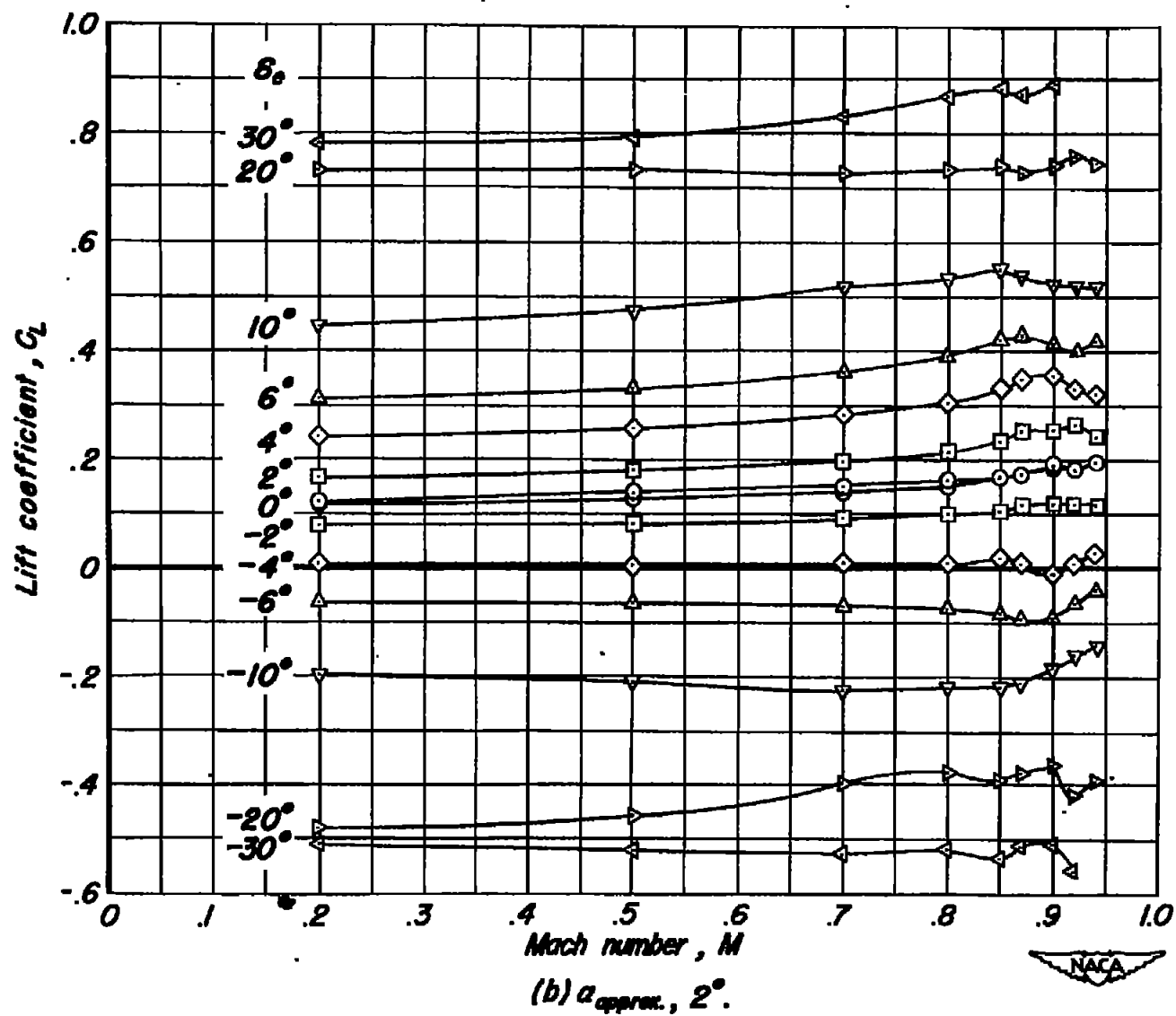
Figure 14.— Continued.

Figure 14.—Continued.

(c) $a_{approx.}$, 4°.

(d) $a_{approx.}$, $6°$.

Figure 14.—Continued.

(e) $a_{approx.}$, $8°$.
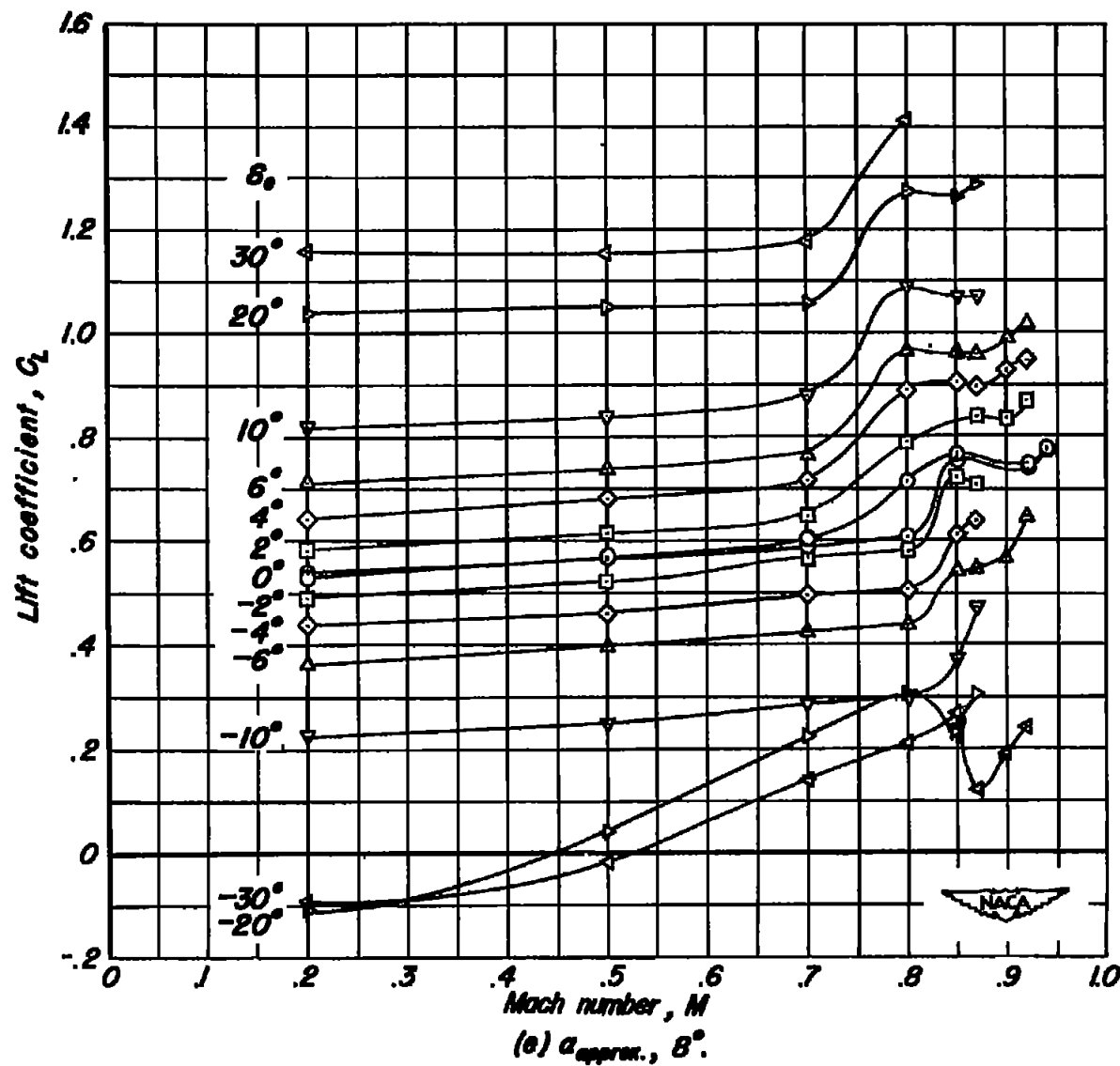
Figure 14.—Concluded.
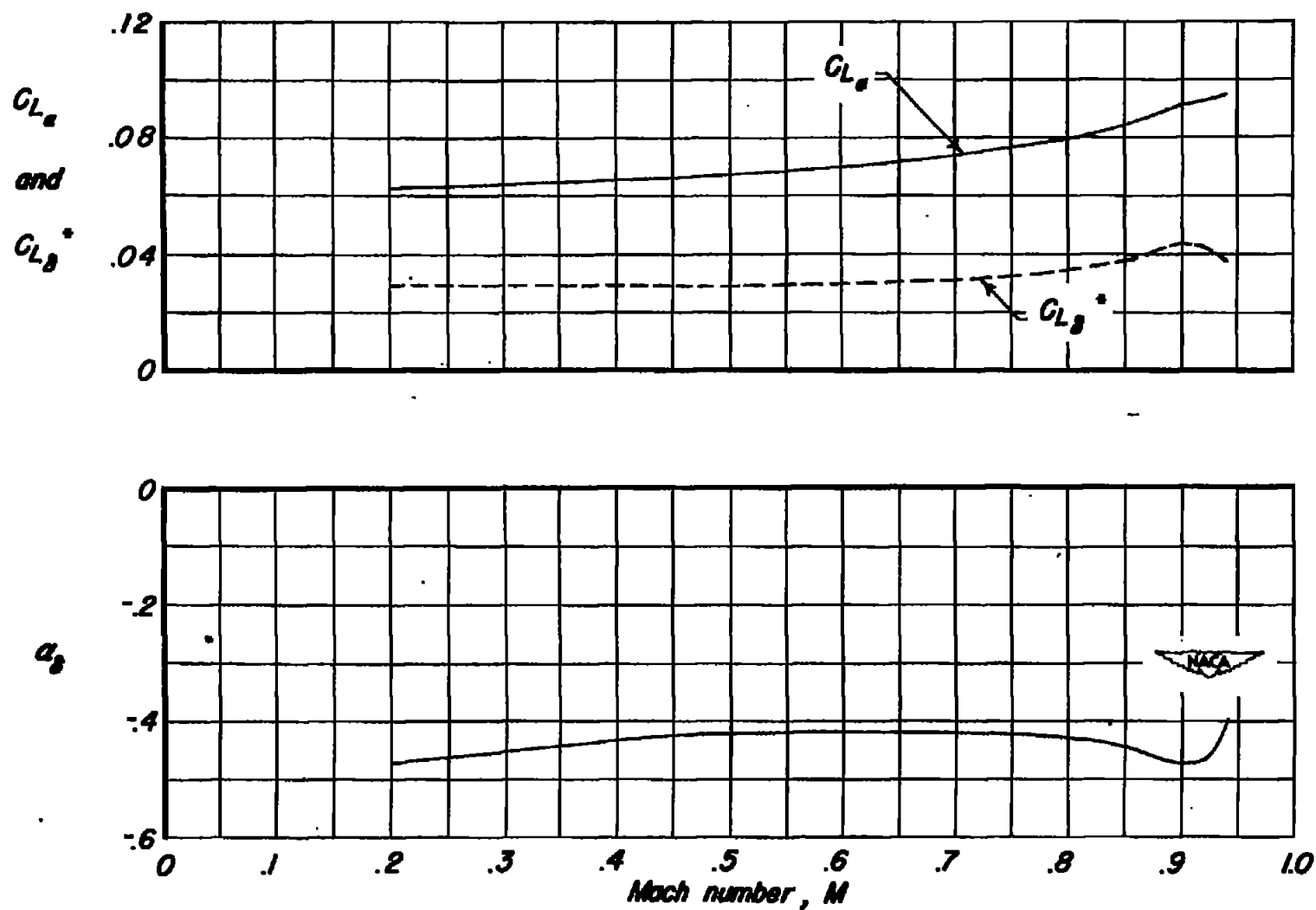
Figure 15.—Variation of lift parameters C_{L_α} , $C_{L_\delta}^*$, and α_δ with Mach number.